NASA Contractor Report 178165

NASA-CR-178165
19860021226

PAN AIR APPLICATION TO THE F-106B

Farhad Ghaffari

VIGYAN RESEARCH ASSOCIATES, INC.
Hampton, Virginia

NASA

National Aeronautics and
Space Administration

Langley Research Center
Hampton, Virginia 23665

NF00193

PAN AIR APPLICATION TO THE F-106B

Farhad Ghaffari

Vigyan Research Associates, Inc.

Hampton, Virginia 23666-1325

SUMMARY

The PAN AIR computer code was employed in the present study to investigate the aerodynamic effects of the various geometrical changes and flow conditions on a configuration similar to the F-106B half-airplane tested in the Langley 30×60-foot wind tunnel. The various geometries studied included two forebodies (original and shortened), two inlet flow conditions (open and closed) and two vortex flap situations (off and on). The attached flow theoretical solutions were obtained for Mach number of 0.08 and angles of attack of 8°, 10°, 12°, and 14°.

In general this investigation revealed that the shortening of the forebody or closing of the inlet produced only a small change in the overall aerodynamic coefficients of the basic F-106B configuration throughout the examined angles of attack. However, closing the inlet of the configuration resulted in a slightly higher drag level at low angles of attack. Furthermore, at and above 10° angle of attack, it was shown that the presence of the vortex flap causes an increase in the total lift and drag. Also, these theoretical results showed the expected reduction in longitudinal stability level with addition of the vortex flap to the basic F-106B configuration.

SYMBOLS AND ABBREVIATIONS

b	=	span
CI	=	Ith combination of basic configuration with inlet, forebody, and vortex flap (Fig. 2)
CODAC	=	Cockpit Oriented Display of Aircraft Configuration
C_D	=	drag coefficient, drag/q_∞ S
C_L	=	lift coefficient, lift/q_∞ S
C_m	=	pitching moment coefficient, (pitching moment)/q_∞ S$\bar{c}$
C_p	=	pressure coefficient, $(p-p_\infty)/q_\infty$
c	=	chord
$\bar{c}$	=	reference chord
M	=	Mach number
$\hat{n}$	=	unit normal vector
p	=	static pressure
PAN AIR	=	panel aerodynamics computer code
q	=	dynamic pressure
S	=	reference area
$\vec{V}$	=	total velocity
$\vec{v}$	=	total perturbation velocity
V_X, V_Y, V_Z	=	X, Y, Z components of the total velocity, respectively
$\vec{W}$	=	total mass flux
$\vec{w}$	=	total perturbation mass flux
X, Y, Z	=	global coordinate axes
x/c	=	fractional distance along chord
α	=	angle of attack, degrees
η	=	fraction of wing theoretical semispan
ρ	=	density

Subscripts

i = inlet

t = tunnel

0 = value at $C_L = 0$

∞ = freestream

INTRODUCTION

In support of the F-106B leading-edge vortex flap project, a half-airplane was tested in the Langley 30×60-foot wind tunnel. Unfortunately, available model and tunnel-constraints caused the tested configuration to differ from that to be used in flight. To gage the effect of the differences, attached flow solutions were obtained using the PAN AIR (panel aerodynamics) computer code [1,2] on a configuration similar to the wind-tunnel model. Though exact agreement is not expected due to the difference in flow type, i.e., attached flow for PAN AIR and vortical for the wind tunnel test, qualitative information should be determinable from this general analytical code. Computational fluid dynamic codes do not currently exist which can handle the complete configuration with vortical flows. The aim in obtaining these theoretical results was to ascertain whether the various geometrical changes or flow conditions actually tested would be reflected in the measured data. The F-106B half-airplane configuration which was wind-tunnel tested consisted of a Case XIV wing (instead of the flight vehicle Case XXIX wing, see reference [3]) mounted on a shortened forebody, open and closed inlet, and with and without a 30° deflected leading-edge vortex flap.

The various geometrical changes were all part of the planned experimental investigation, with the exception of the forebody. The original forebody on the full-scale model was modified as a result of a compromise which had to be made between the aerodynamic load center of the half-airplane and the center of gravity of the tunnel ground board support. This compromise — brought about by model support considerations — fixed the location where the half-airplane could be positioned on the tunnel ground board. However, it was

subsequently determined that at high angles of attack ($\alpha > 30^\circ$), the original forebody of the half-airplane approaches too close to the tunnel wall, where the flow may no longer be uniform due to the wall interference effects. Therefore, to minimize these interference effects the fuselage forebody was shortened. The photograph in Fig. 1 shows the test setup for the F-106B half-airplane with the modified forebody and leading edge vortex flap in place.

The flexibility and geometrical generality of the PAN AIR higher-order panel code (linear source and quadratic doublet distribution) provides the user with a great deal of freedom and capability in modeling potential flow problems. This study attempts to exercise the various capability of the code such as modeling the actual surfaces of the complete configuration including different inlet flow condition, wing vortex-flap combination and off-body flow field survey. Applications of this code to many different aircraft configurations have been well documented (i.e., see references [4-7]) and demonstrate the inherent accuracy of this method. The PAN AIR theoretical representation of the various studied geometries on the F-106B included two forebodies (original and shortened), two leading-edge vortex flap situations (on and off), and two inlet flow conditions (open and closed). These eight different combinations are indicated in the solution chart shown in Fig. 2. Theoretical solutions were obtained for each combination at a Mach number of 0.08 and angles of attack of 8, 10, 12, and 14°. These solutions include second-order surface pressure coefficients, forces, moments, and off-surface flow fields around the leading edge of the wing (or vortex flap) at five different span stations. It should be noted that these solutions are obtained for free air.

GEOMETRY PREPARATION

This chapter introduces and gives demonstrations of the different computer codes employed either to display or generate the various geometry components used in the present analysis.

Basic F-106B Configuration

The original F-106B geometry was defined using approximately 3200 grid points which, once converted into surface panels, were well in access of the PAN AIR code limitation. As a result, the number of grid points were reduced to about 900, without introducing any significant changes to the original airplane geometry. This geometry manipulation was performed by using a computer code called GEOMX [8]. The new set of grid points were then used in another computer code called CODAC (Cockpit Oriented Display of Aircraft Configurations [9]) to display the configuration with its hidden lines removed. Figure 3 illustrates an isometric view of the surface panels associated with the reduced number of grid points for the F-106B wing-fuselage combination. The PAN AIR input geometry consisted of 401 panels for the fuselage and 464 panels for the wing.

Shortened Forebody

The surface panel representation of the shortened forebody was generated from three measured curves, defined by a small number of grid points. These curves were located along the upper and lower surfaces of the vertical plane of symmetry and along the waterline, as shown schematically in Fig. 4. Obviously, the number of grid points available to describe these curves was

deficient for both good curve definition and subsequent generation of the required surface panels. However, this problem was circumvented by making an assumption that the desired curves were cubics and the surface bi-cubical. A further assumption was that this surface would blend with the well-defined fuselage surface panels and would pass through all the measured grid points. This principle was applied and the surface panels for the shortened forebody were generated by employing the geometry capability of PATRAN-G [10], developed by PDA. The three-view computer drawing of the constructed surface panels transposed over the original forebody is shown in Fig. 5. Also, the isometric view of the fuselage with the shortened forebody is shown in Fig. 6 to illustrate the relative size change by the forebody modification.

Leading-Edge Vortex Flap

The PAN AIR input geometry for the wing was modified to include the 30° deflected leading-edge vortex flap. Although the vortex flap tested on the half-airplane was extended to the wing tip section (Fig. 1), no geometrical data was available to model the vortex flap surface panels beyond 94% of the wing semispan. Figure 7 shows the surface panels for the wing-fuselage combination with the 30° deflected leading-edge vortex flap. Furthermore, Fig. 8 shows an isometric view of the streamwise cuts through the wing vortex-flap combination. The PAN AIR input geometry consisted of 568 panels for the wing with the leading edge vortex flap.

Survey Networks

The flow field survey networks used in present investigation were vertical planes at five spanwise stations, and were also generated by

PATRAN-G. Due to the great interest in establishing the geometrical and flow condition influence on the velocity field solutions around the wing leading edge, the nose region of the wing geometry was enclosed by these networks. Furthermore, since the stagnation point is very sensitive to flow condition changes and it is often on the lower surface, that part of the wing nose region was emphasized. The networks had the same interior shape as the input geometry for a particular wing section and stood off from the surface approximately 0.1% of the wing root chord. An isometric view of a typical survey network positioned on the wing is shown in Fig. 9. Furthermore, the cross-sectional view of the same typical survey network is shown in Fig. 10. The same principle was applied to generate the corresponding survey networks for the vortex flap leading-edge. The cross-sectional view of a typical survey network constructed to examine the flow field around the leading-edge of the vortex flap is shown in Fig. 11.

PAN AIR UTILIZATION

In addition to modeling the external shape of the various configurations of interest, the present study utilized several built-in features of the PAN AIR code. These included the Influence Coefficient (IC) update and inlet flow simulation. The IC-update capability provides for the computation of the velocity field solutions on the survey networks in an expeditious manner. Furthermore, the IC-update capability of the code enables one to examine configurations which differ from the ones already processed in a limited fashion with respect to geometry or boundary conditions. In this economically

5

efficient process a configuration surface is partitioned into several networks, with one or more tagged "updatable" in the original submission. The subsequent run, with any change (i.e., size, location, or boundary conditions) in the updatable networks can utilize some of the unaffected calculations which have been performed and saved from the original execution.

Regarding inlet flow simulation, the inlet flow conditions investigated were those measured during the wind-tunnel test, namely, closed and open. For the closed inlet, an impermeable surface was employed at the inlet opening face to prevent the flow from entering through the inlet duct. Whereas, for the open inlet, a dimensionless mass flux were specified in terms of the freestream value. It should be noted that for the latter case, two probes were located inside the inlet just behind the opening face of the half-airplane model to measure the velocity field. The simple process of developing corresponding mass flux in a dimensionless form is given next.

The total mass flux $\vec{W}$ in PAN AIR theory document [2] is defined as:

$$\vec{W} = (\rho/\rho_\infty) \cdot \vec{V}$$ (1)

where ρ and ρ_∞ are the local and freestream fluid density respectively, and $\vec{V}$ is the fluid total velocity. For incompressible flow ($\rho = \rho_\infty$), the perturbation mass flux $\vec{w}$ is equal to the perturbation velocity $\vec{v}$; the mass flux boundary condition is then equivalent to that of normal velocity at the surface. Hence,

$$\vec{W} = \vec{V} = \vec{V}_\infty + \vec{w} = \vec{V}_\infty + \vec{v}$$ (2)

6

where $\vec{V}_{\infty}$ is the total fluid freestream velocity. Furthermore, let β be the unknown amount of the mass flux through the inlet face, therefore,

$$(\beta) = \vec{W} \cdot \hat{n} = (\vec{V}_{\infty} + \vec{w}) \cdot \hat{n} = (\vec{V}_{\infty} + \vec{v}) \cdot \hat{n} \tag{3}$$

The above equation relates the total mass flux to the total fluid velocity. Applying this equation to the inlet opening and a tunnel station away from the test section where the flow is uniform (i.e., $\vec{v} = 0$). The resulting ratio becomes

$$\frac{\beta_i}{\beta_t} = \frac{(\vec{W}_i) \cdot \hat{n}}{(\vec{W}_t) \cdot \hat{n}} = \frac{(\vec{V}_{\infty} + \vec{v}_i) \cdot \hat{n}}{\vec{V}_t \cdot \hat{n}} \tag{4}$$

where the subscripts i and t denote the flow conditions at the inlet face and a tunnel station away from the test section. The right-hand side of the above equation is the ratio of the total fluid velocity measured at the open inlet to that of the tunnel freestream velocity. At 8° angle of attack, the average total velocity measured by the two probes at the inlet face was 101.13 ft/sec. based on the full-scale tunnel freestream of 90.0 ft/sec. As a result

$$\frac{\beta_i}{\beta_t} = \frac{101.13}{90.0} = 1.12 \tag{5}$$

This dimensionless total mass flux was specified in the PAN AIR code to simulate the amount of flow entering through the inlet face. Although this mass flux ratio could vary slightly with angle of attack, it is assumed that it remains constant throughout the examined angles of attack range in the present study.

7

RESULTS AND DISCUSSIONS

The PAN AIR theoretical solutions for the various studied geometries on the F-106B configuration include two forebodies (original and shortened), two leading edge vortex flap situations (on and off), and two inlet flow conditions (open and closed). Although, total of eight different combinations (Fig. 2) were investigated, due to space limitation, only four will be discussed in this report. These four combinations are selected such that the aerodynamic effects resulting from 1) presence of vortex flap, 2) shortened forebody, and 3) closing of the inlet, could be addressed through a direct wing pressure comparisons with the ones obtained for the basic F-106B configuration. Furthermore, the PAN AIR theoretical chordwise pressure distributions were obtained for fourteen stations along the wing semispan, however, only five selected typical stations will be presented here for each combination, as shown in Fig. 12. In addition to the wing pressure comparisons, the total aerodynamic coefficients of the modeled configurations as well as a typical leading edge velocity field surveyed for each combination at a station (η = .24) nearest to the fuselage will also be discussed. This station was selected because of the maximum aerodynamic effects resulting from the various studied combinations, in particular from the inlet and forebody, occurred around the leading edge portion of this station. The velocity field plots presented in this report are the resultant velocity vectors obtained from vectorial addition of the axial (V_X) and the upwash (V_Z) velocity components which have been computed, by the PAN AIR code, at the center point of each panel in a particular survey network. As a result, the plotted velocity field solutions do not include any contribution from the sidewash

8

(V_Y) velocity component. Furthermore, it should be noted that the semispan locations at which the leading edge velocity field have been surveyed differ from the stations where the wing (or vortex flap) chordwise pressures have been calculated, because PAN AIR calculates the pressures at the center point of each panel, whereas, the survey networks are aligned with the input geometry of the wing and/or flap section. The theoretical solutions were obtained for each combination at Mach number of 0.08 and angles of attack of 8°, 10°, 12°, and 14° these theoretical calculations were all based on second-order pressure rule.

Basic F-106B Configuration

To assess the aerodynamic effects of various geometrical changes or inlet flow conditions in the present study, a basic F-106B geometry was chosen to serve as a baseline configuration. This configuration is composed of the original forebody, open inlet, and no leading-edge vortex flap. The surface panels representation of this configuration modeled by the PAN AIR was shown earlier in Fig. 3.

The effect of angles of attack on the wing chordwise pressure distribution for the basic F-106B configuration is shown in Fig. 13, for Mach number of 0.08. In this figure, the chordwise distance along each wing semispan have been nondimensionalized with respect to the wing local chord. Figure 14 shows the total aerodynamic characteristics for the basic F-106B configuration. It should be noted that all the theoretical drag coefficients presented in this report have been adjusted to include the experimental value of drag at zero lift (C_{DO}) of 0.015. Also, the wing leading-edge velocity

field solutions obtained at the fractional theoretical semispan location of $\eta = 0.24$ for the two extreme angles of attack of 8° and 14° are shown in Fig. 15.

Effect of Shortened Forebody

This section is designed to address the aerodynamic effects of the forebody modification on the F-106B configuration. The wing chordwise pressure distributions computed by the code for the basic F-106B configuration with the original and shortened forebody are shown in Fig. 16. As it can be seen from the figure, the forebody modification do not have a significant effect on the wing pressure distribution throughout the examined angles of attack. Figure 17 also shows the insensitivity of the total longitudinal aerodynamic characteristics to the forebody modification. Furthermore, the wing leading-edge velocity field solutions computed for 8° and 14° angles of attack, $\eta = 0.24$, are shown in Fig. 18. A comparison of this figure with Fig. 15, indicate that no considerable change is occurring on the wing leading-edge velocity field solutions as a result of the forebody modification.

Effect of the Inlet Flow Condition

As part of the present study, it was important to investigate the aerodynamic effects of the closed inlet flow conditions on the neighboring surfaces. For this purpose, no flow through boundary condition was imposed on the inlet face network. The wing chordwise pressure distribution computed by the PAN AIR code for the basic F-106B configuration with open and closed inlet are shown in Fig. 19. It is evident from this figure, that at low angles of attack (8° and 10°), the closing of the inlet produces a slight change in the

10

wing pressure distribution only at the most inboard station (η = .225).
However, this effect appears to vanish at higher angles of attach (12° and
14°). Outboard of this station (η = 0.225), no considerable change in the
wing pressure distribution can be noticed throughout the examined angles of
attack. Furthermore, Fig. 20 shows the effect of inlet flow condition on the
total longitudinal aerodynamic characteristics of the basic F-106B
configuration to be small. This minimal effect can also be seen from a
comparison of the wing leading-edge velocity field calculations shown in Figs.
21 and 15.

Effect of Leading-Edge Vortex Flap

Significant changes are to be expected in the leading edge region with
the addition of a vortex flap. The basic F-106B geometry was modified to
include the 30° deflected leading-edge vortex flap. The PAN AIR surface panel
representation of the configuration is shown in Fig. 4. A single component
(comprised of an upper and lower surface network) approach was chosen to model
the wing vortex-flap combination. The forward portion of the basic wing lower
surface geometry was changed dramatically as a result of the vortex flap
thickness being attached there (see Fig. 8).

The chordwise pressure distributions on the wing vortex-flap combination,
as well as the basic F-106B configuration, are shown in Fig. 22. (Note that
the x/c values of less than zero are on the flap.) At the wing most inboard
station (η = 0.225), the presence of the vortex flap apparently has only a
slight effect on the basic wing pressure distribution. This could be well due
to the small local chord in the vortex flap apex area. However, outboard of

11

this station, the basic wing pressure distribution, especially the upper surface, has change dramatically. For example, at $\eta = 0.666$, this figure shows the very interesting results of a double suction peak at and above 10° angle of attack. Though this is attached flow, similar double suction peaks were measured experimentally as shown in reference [11]. In addition, this figure reveals that the presence of the vortex flap reduces the wing leading edge suction peak without producing a significant change on the wing lower surface pressure distribution except around the tip where the contribution of the flap thickness to the overall wing sectional thickness becomes large (see Fig. 8).

The effect of the presence of the leading-edge vortex flap on the longitudinal aerodynamic characteristics of the basic F-106B configuration is presented in Fig. 23. It is interesting to note that at 8° angle of attack, this figure shows that no considerable change is occurring in neither lift or drag, however, at higher angles of incidence the vortex-flap presence causes an increase in both lift and drag coefficients. Furthermore, the results on the pitching moments indicate that adding the vortex flap to the basic F-106B configuration bring about the expected reduction in the slope of the longitudinal stability curve $(dC_m/d\alpha)$. Also, the vortex flap leading-edge velocity field solutions computed for the two extreme angles of attack of 8° and 14°, at $\eta = 0.24$, are shown in Fig. 24. It appears that, 8° angle of attack, the leading-edge vortex flap is aligned with incoming flow. This effect can also be noticed at the other semispan stations by examining the flatness of the chordwise pressure distribution on the flap surface in Fig. 22.

CONCLUDING REMARKS

The results obtained from the PAN AIR code indicated that the shortening of the forebody did not have significant effect on the wing pressure distributions throughout the examined angles of attack. Furthermore, the insensitivity of the forebody modification on the total longitudinal aerodynamic characteristics of the basic configuration was also disclosed.

At low angles of attack, the results showed that the closing of the inlet caused a slight change in the wing chordwise pressure distribution only at the leading-edge portion of the most inboard station. However, this effect appeared to vanish at higher angles of incidence. In addition, this minimal effect was also reflected in the total longitudinal aerodynamic characteristics of the basic configuration.

As expected, the presence of the leading-edge vortex flap resulted in the most drastic change in the wing pressure distributions, expecially around the leading-edge area. Though attached flow, these solutions showed a double suction peak (one for the flap leading edge and the other for the wing leading edge) at and above 10° angle of attack. It was also evident that, the aerodynamic effects of the presence of the vortex flap on the basic F-106B configuration become more pronounced with increasing angle of attack. Furthermore, the results on the pitching moments indicate that adding the vortex flap to the basic configuration provides a reduction in the slope of the longitudinal stability curve.

REFERENCES

[1] Magnus, A. E.; and Epton, M. A.: PAN AIR a Computer Program for Predicting Subsonic or Supersonic Linear Potential Flows About Arbitrary Configurations Using a Higher Order Panel Method. Volume 1, Theory Document (Version 1.0), NASA CR-3251, May 1980.

[2] Sidwell, K. W.; Baruah, P. K.; and Bussoletti, J. E.: PAN AIR a Computer Program for Predicting Subsonic or Supersonic Linear Potential Flows About Arbitrary Configurations Using a Higher Order Panel Method. Volume 2, User's Manual (Version 1.0), NASA CR-3252, May 1980.

[3] Huebner, L. D.: The Detailed Surface Geometry Development of the Convair F-106B with Vortex Flaps: Initial Aerodynamic Application. AIAA Mid-Atlantic Student Conference, April 19-20, 1985, Pennsylvania State University.

[4] Cenko, A.: PAN AIR Application to Complex Configurations. J. of Aircraft, Vol. 20, No. 10, October 1983.

[5] Dehart, J. H.; Cramer, K. R.; and Miller, S.: Application of PAN AIR Production Code to a Complex Canard Wing Configuration. AIAA 83-0009.

[6] Chen, A. W.; and Tinoco, E. N.: PAN AIR Applications to Aeropropulsion Integration. J. of Aircraft, Vol. 21, No. 3, March 1984.

[7]   Cenko, A.; Tinoco, E. N.; Dyer, R. D.; and Dejongh, J.:   PAN AIR
       Applications to Weapons Carriage and Separation.   J. of Aircraft, Vol.
       18, No. 2, February 1981.

[8]   Hall, J. F.; Neuhart, D. H.; and Walkley, K. B.:   An Interactive Program
       for Manipulation and Display of Panel Method Geometry.   NASA CR-166098,
       March 1983.

[9]   Bingel, B.; and Hammond, D.:   Cockpit Oriented Display of Aircraft
       Configurations (CODAC).   User's Manual, Computer Science Corporation,
       Hampton, VA,   January 1986.

[10] PATRAN-G Release 1.5 User's Guide.   PDA Engineering, Santa Anna, CA,
       March 1984.

[11]Yip, L. P.:   Investigation of Vortex Flaps on the F-106B Airplane
       Configuration in the 30 by 60 Foot Wind Tunnel.   NASA CP 2417, Vol. II,
       1986, pp. 201-226.

15
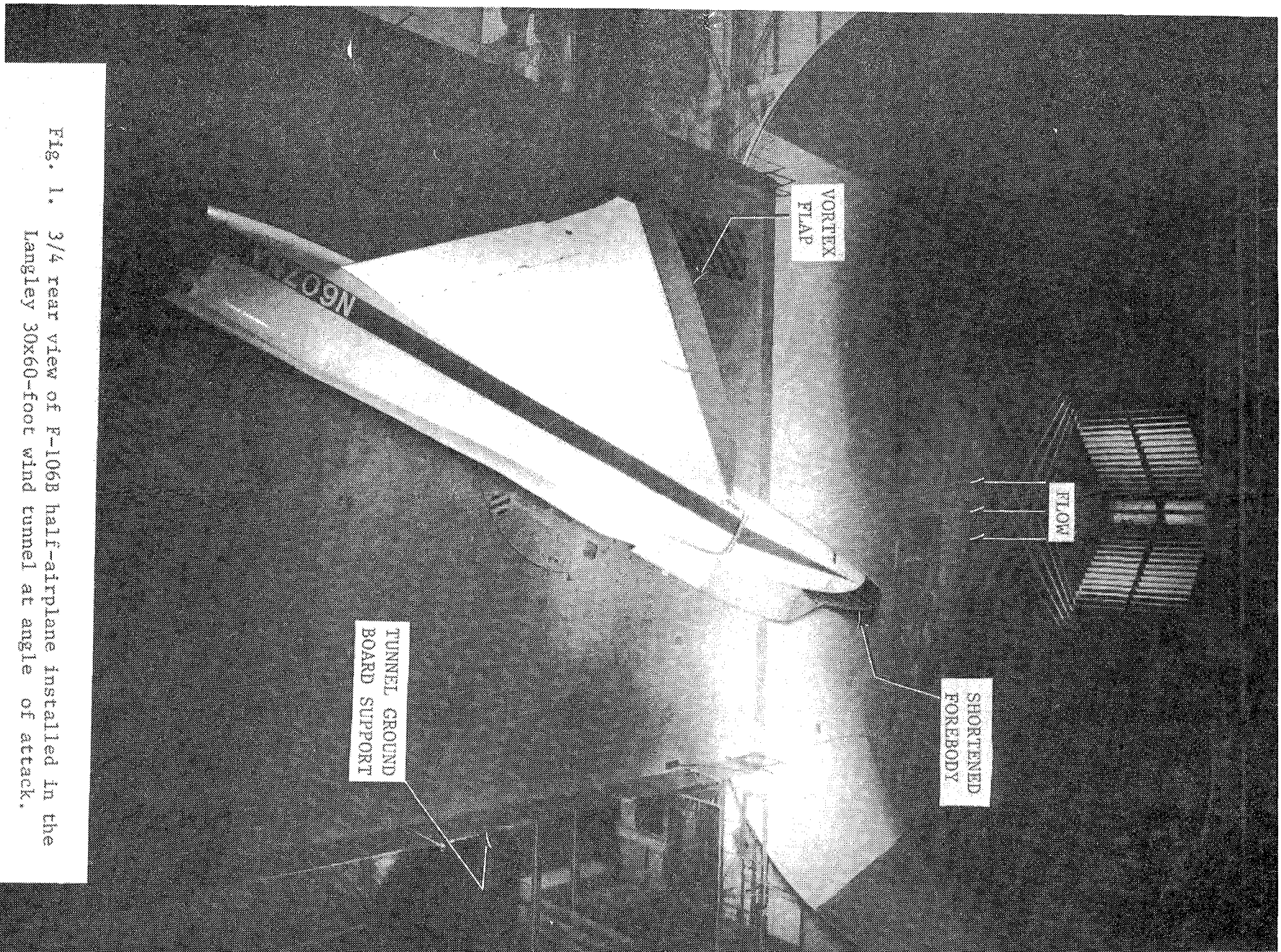
Fig. 1. 3/4 rear view of F-106B half-airplane installed in the Langley 30x60-foot wind tunnel at angle of attack.

VORTEX FLAP

FLOW

TUNNEL GROUND BOARD SUPPORT

SHORTENED FOREBODY

16
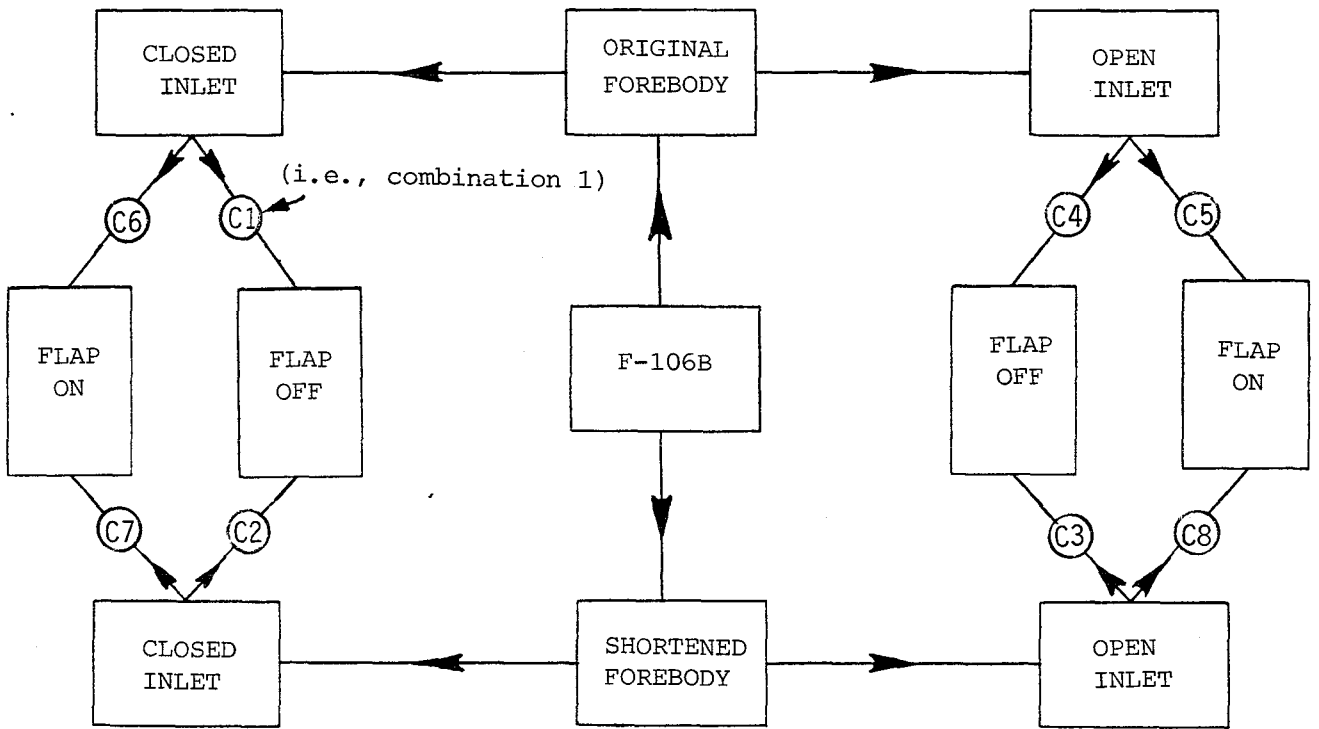
Fig. 2. Various geometrical combinations analyzed using PAN AIR.
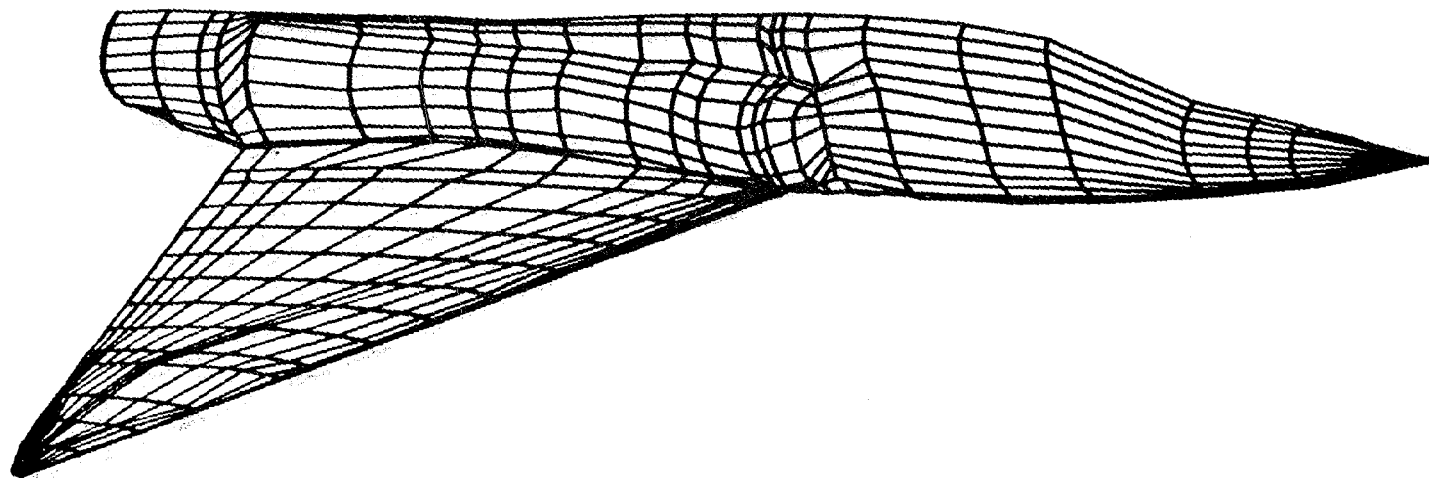
Fig. 3. Isometric view of the F-106B wing-fuselage combination.
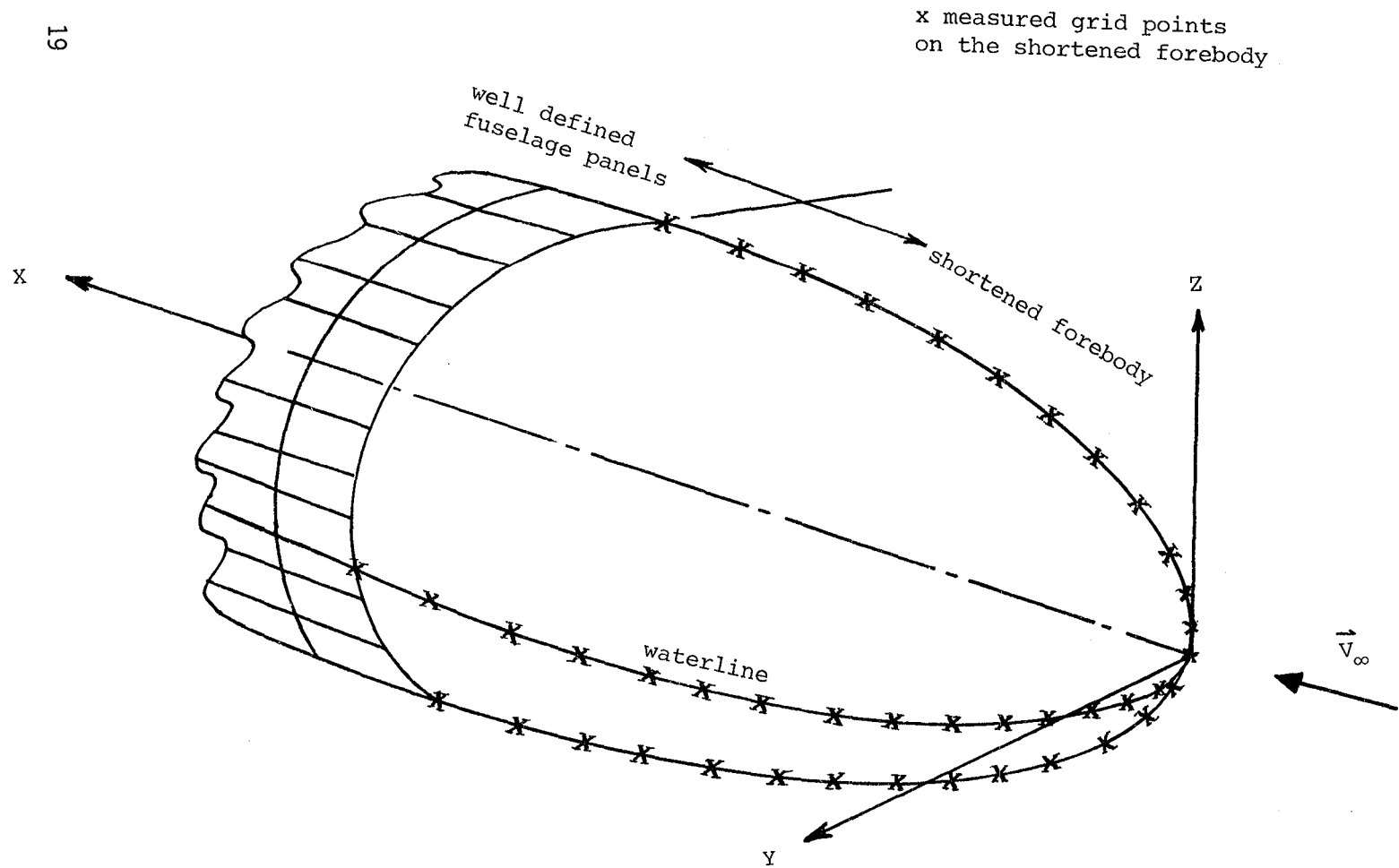
Fig. 4. Schematic view of the measured grid points on the shortened forebody.
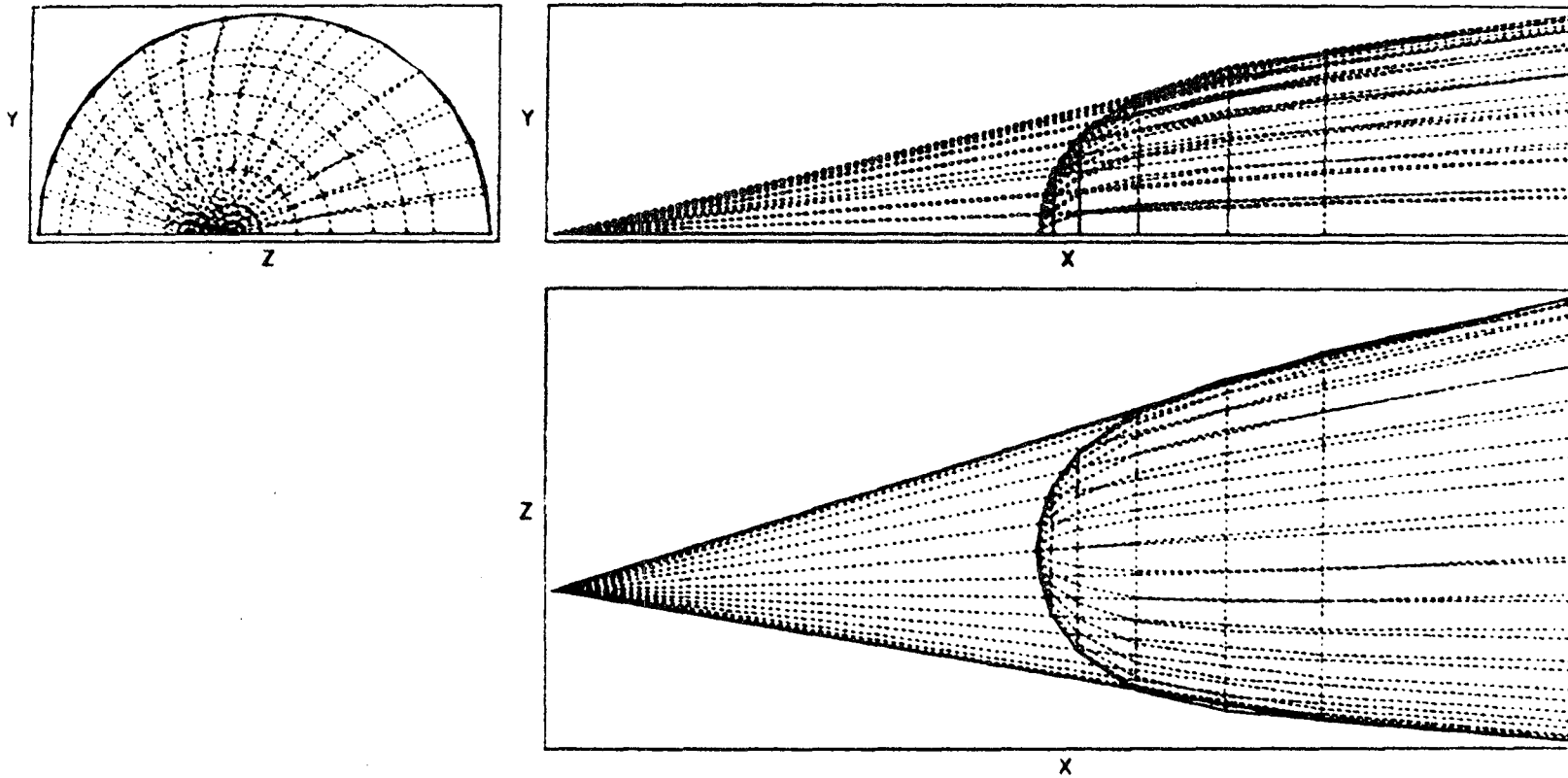
Fig. 5. Shortened forebody transposed over the original.
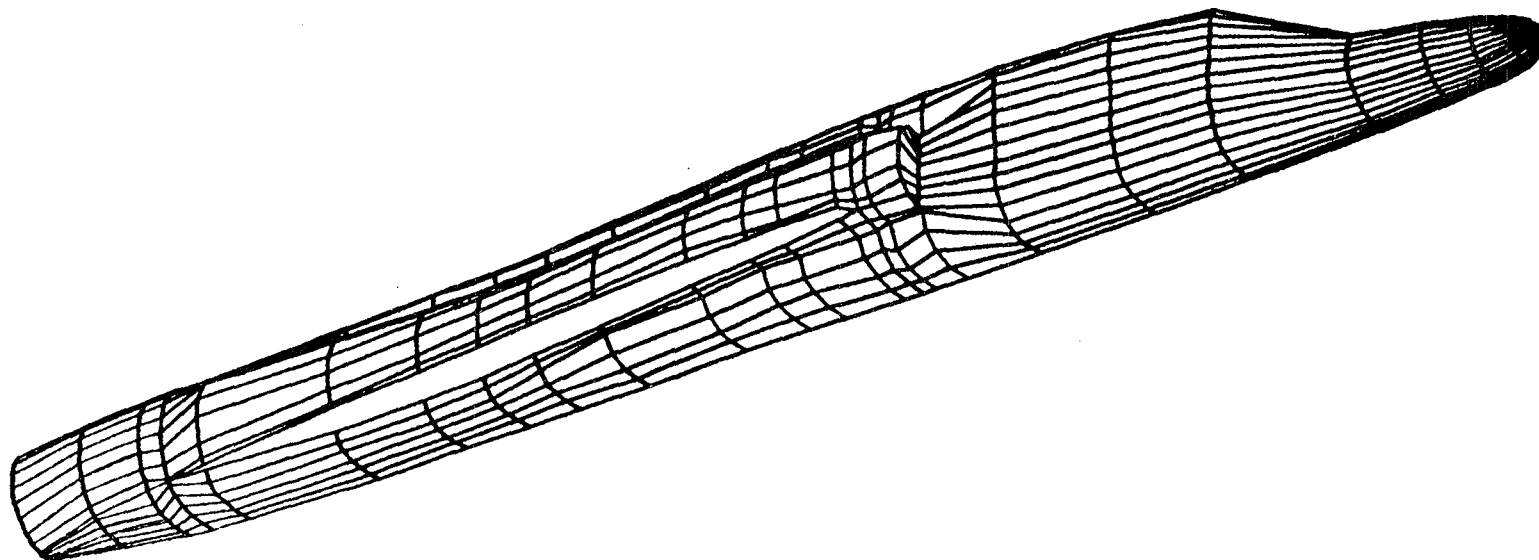
Fig. 6. Isometric view of the F-106B fuselage with shortened forebody.
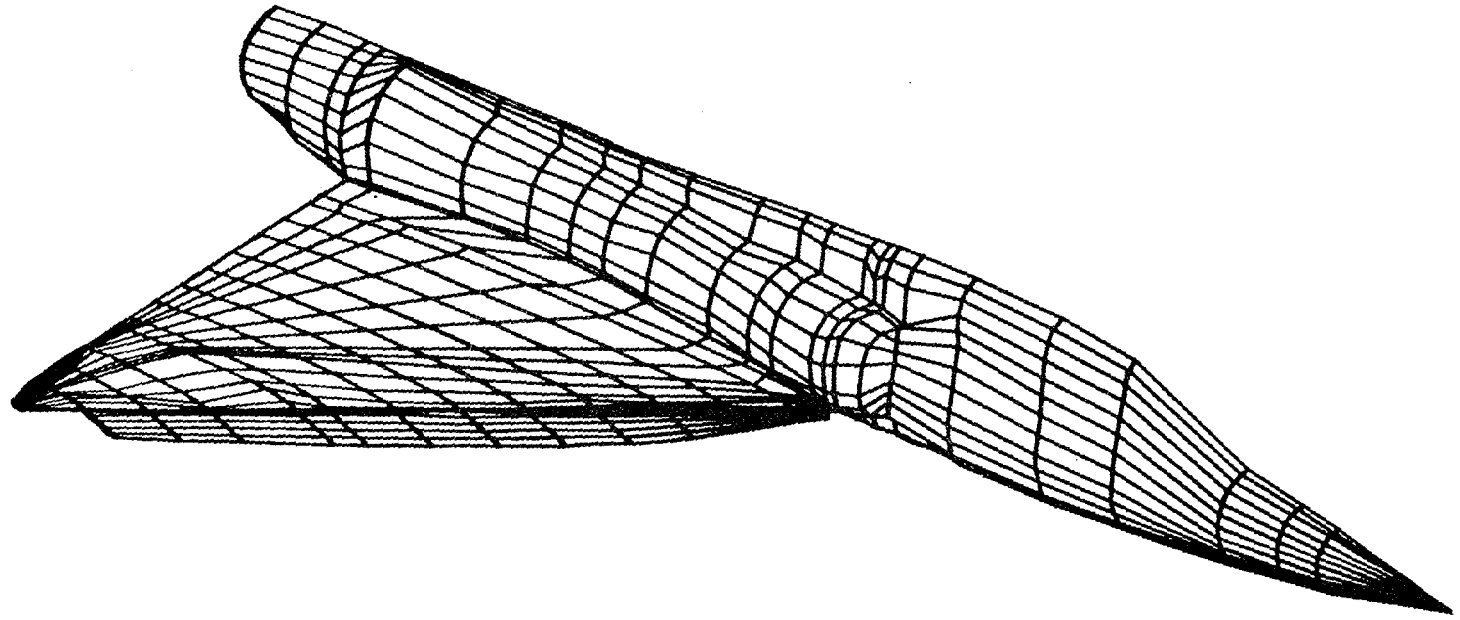
Fig. 7.   F-106B wing-fuselage surface panels with 30° deflected vortex flap.

Fig. 8. Streamwise cuts through the wing-flap combination.
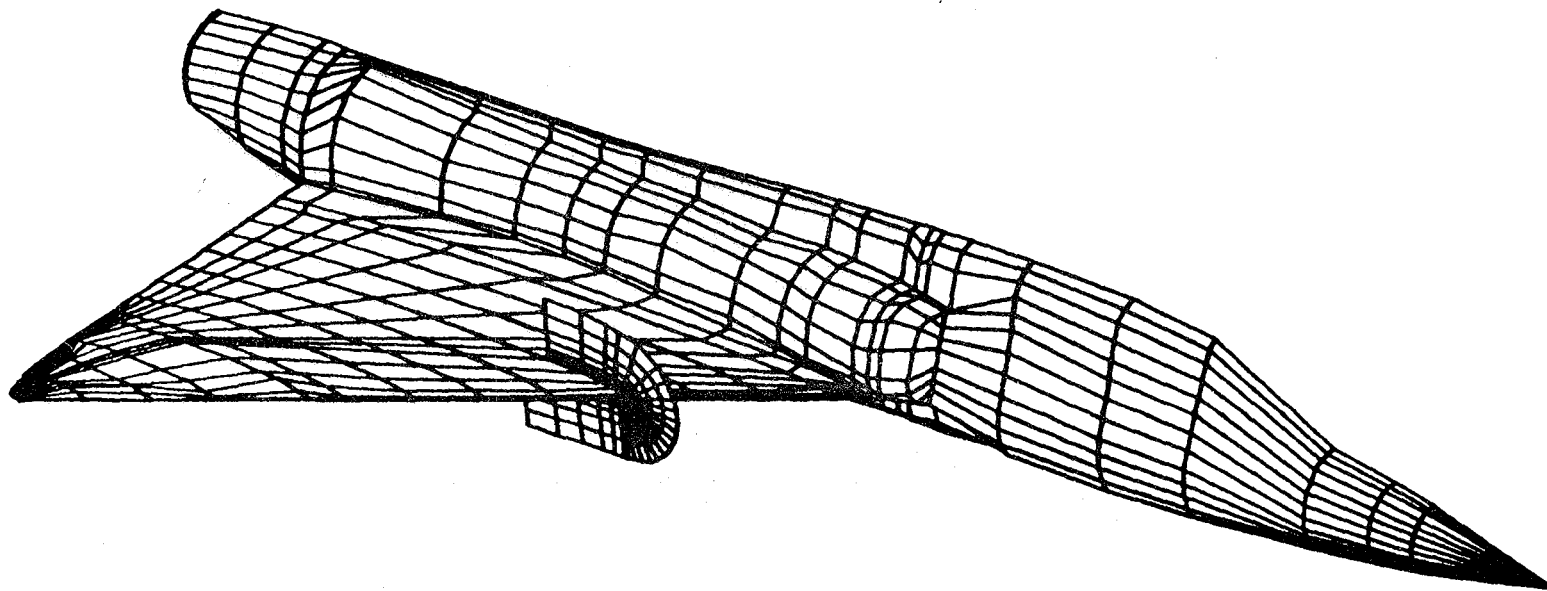
Fig. 9. A typical flow field survey network on the
basic F-106B configuration.
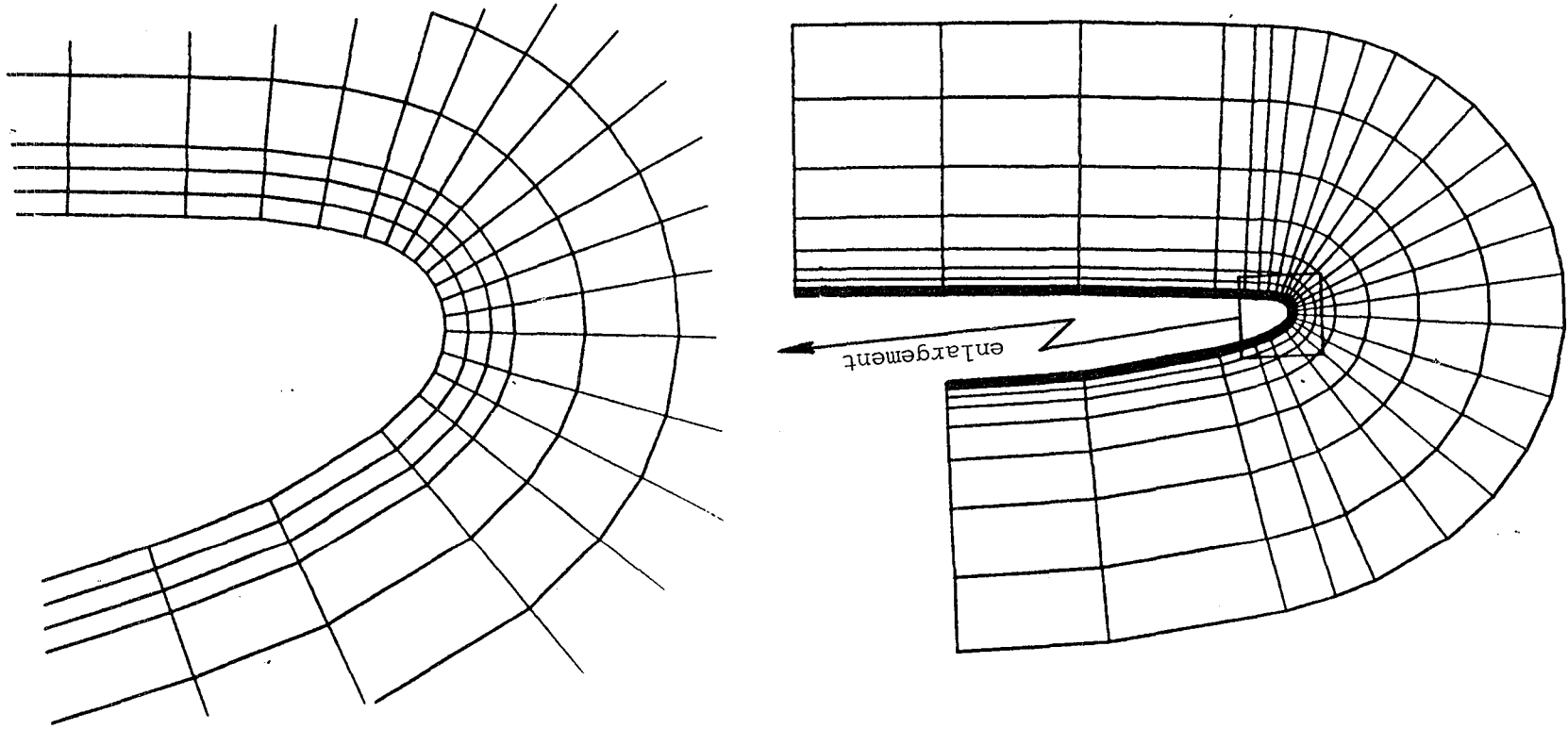
Fig. 10. Cross-sectional view of a typical wing flow field survey network.

enlargement

enlargement
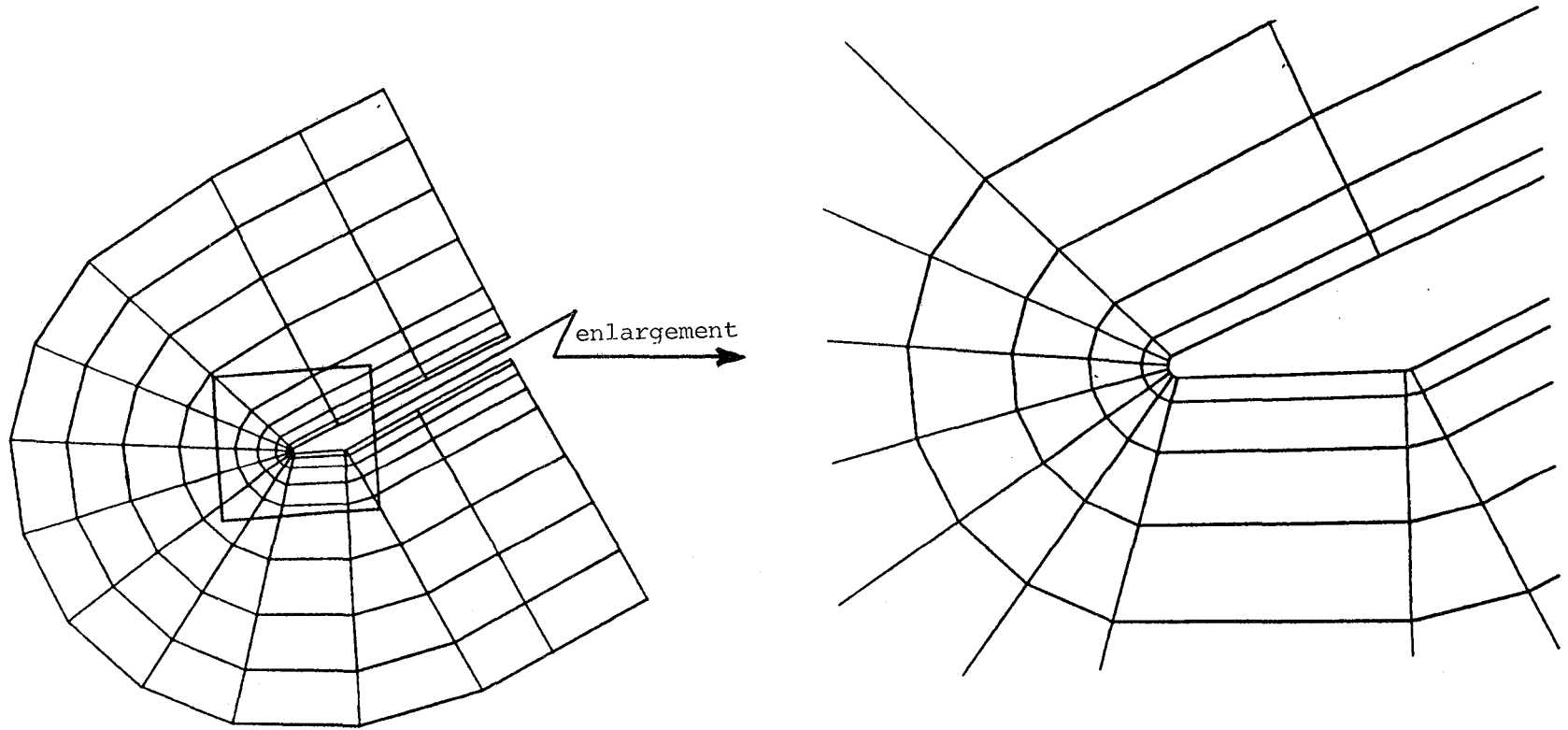
Fig. 11. Cross-sectional view of a typical vortex-flap
flow field survey network.

$\eta = .225$

$= .335$

$= .469$

$= .666$

$= .911$
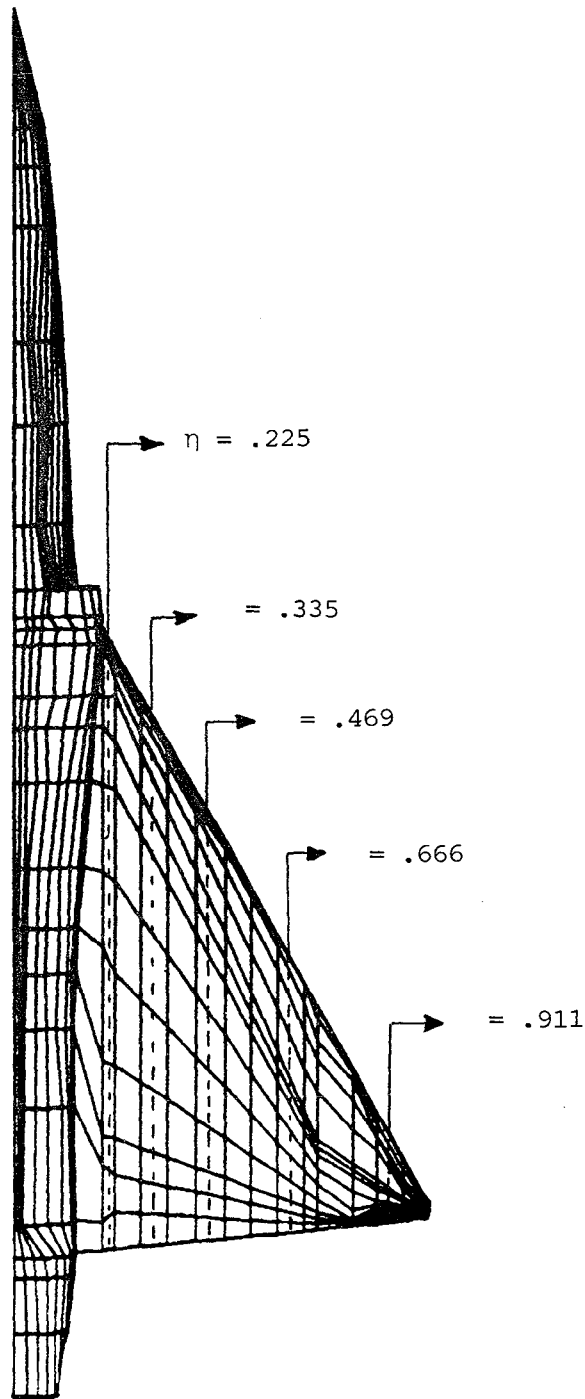
Fig. 12. Selected span stations for the wing chordwise pressure study.
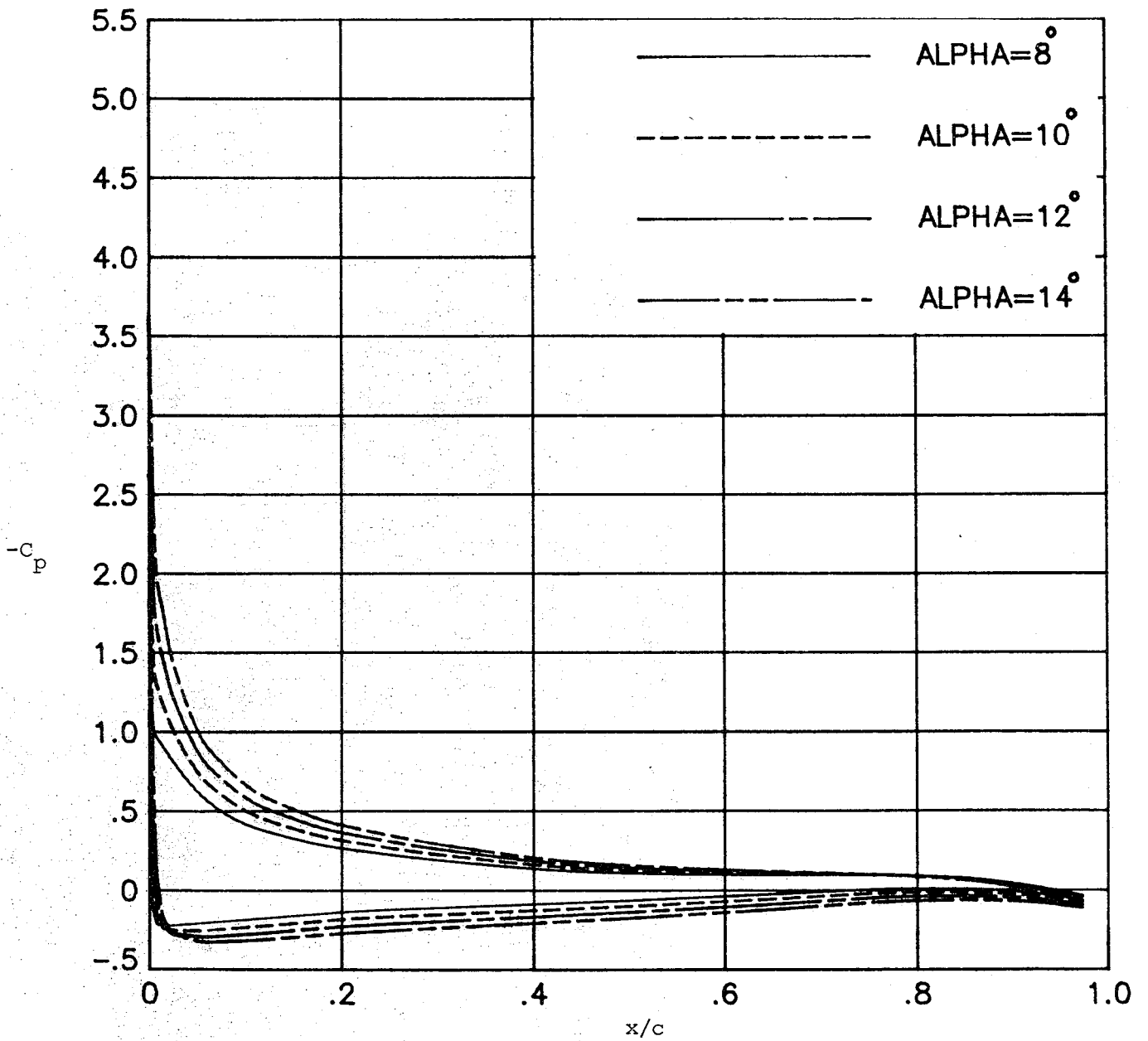
(a) $\eta = 0.225$

Fig. 13. Effect of angle of attack on the wing chordwise pressures for the basic F-106B configuration; $M_{\infty} = 0.08$.

28
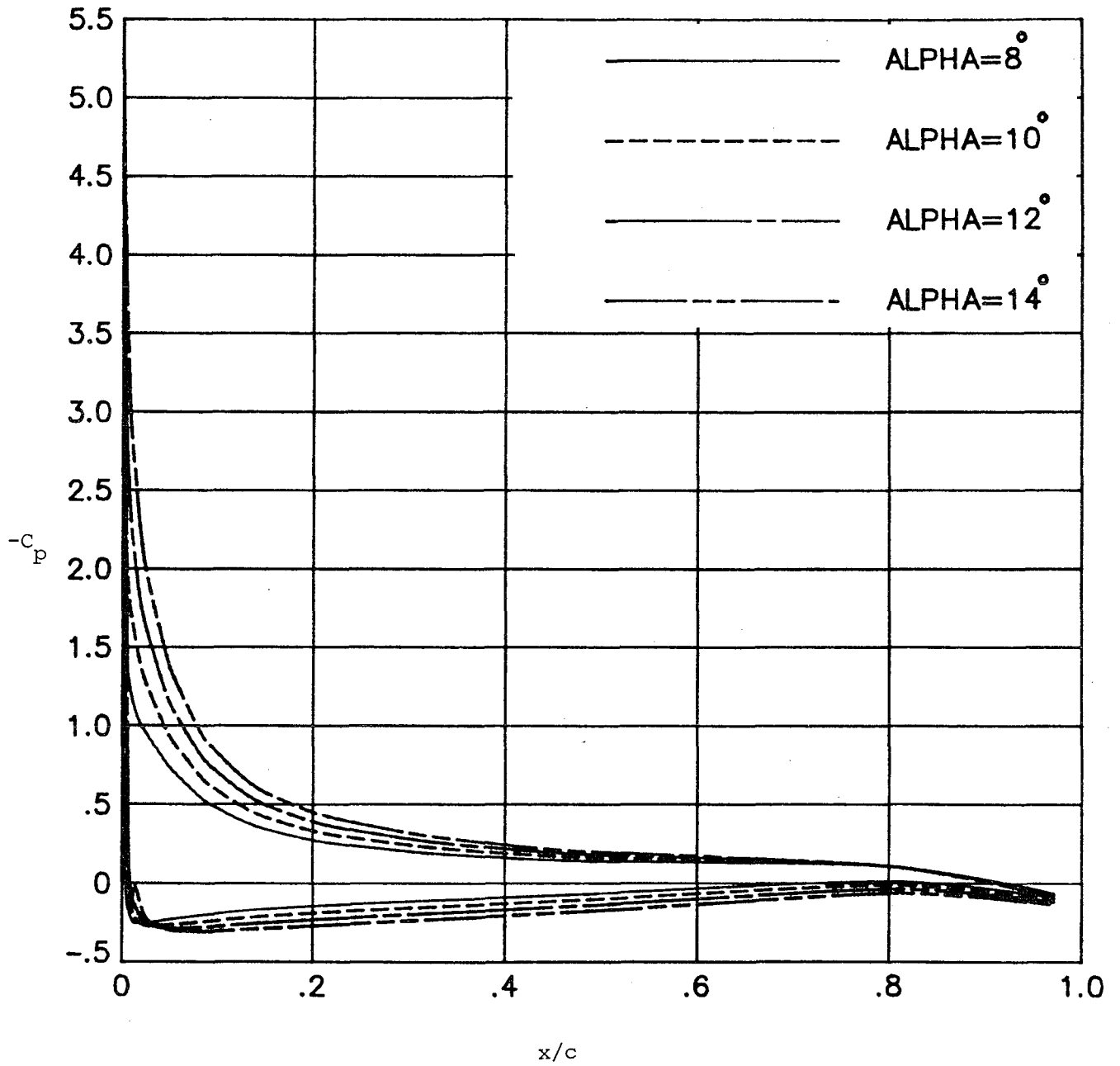
(b) η = 0.335

Fig. 13. Continued.

(c) $\eta = 0.469$

Fig. 13. Continued.

30

(d) $\eta = 0.666$

Fig. 13. Continued.

31
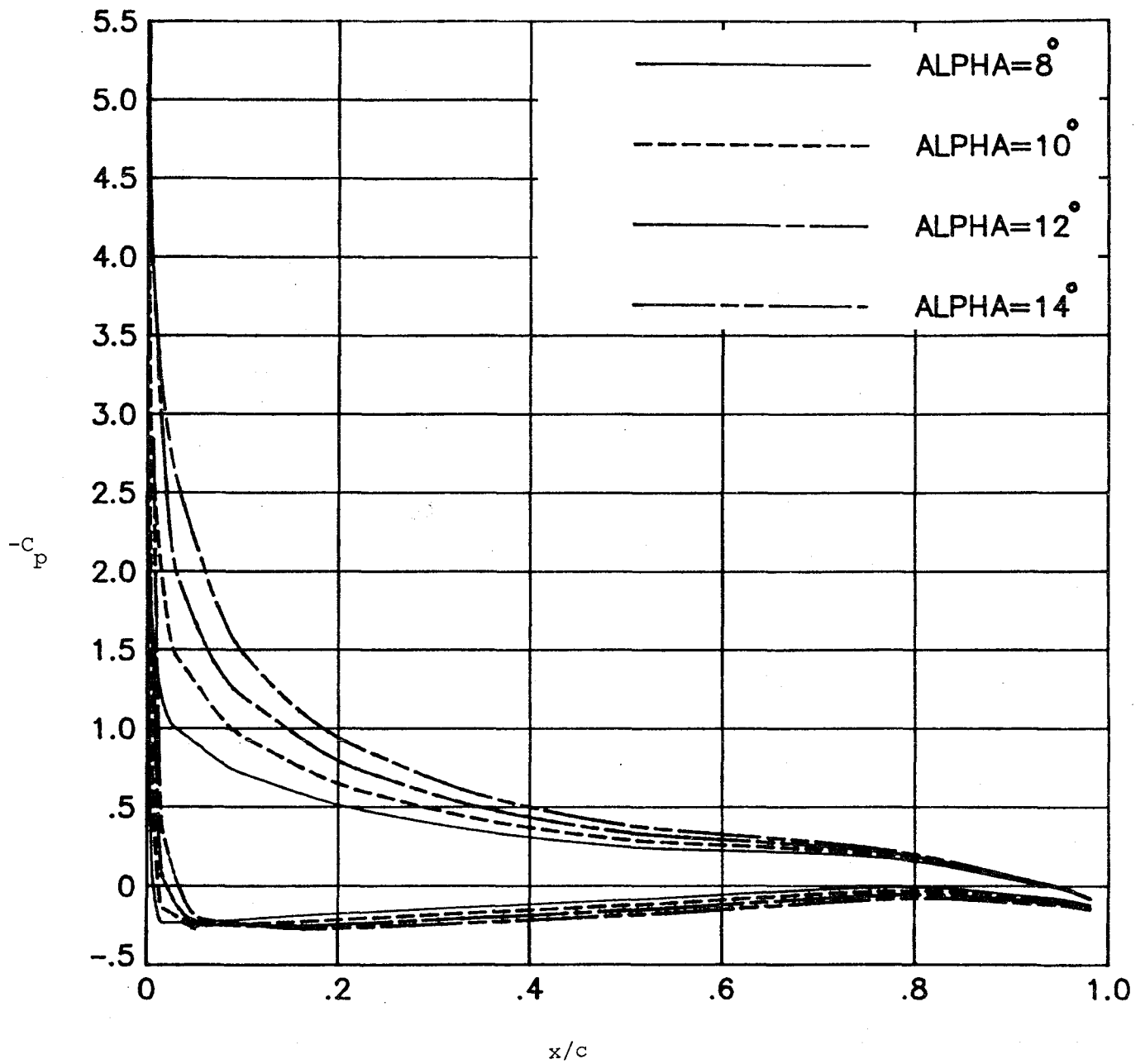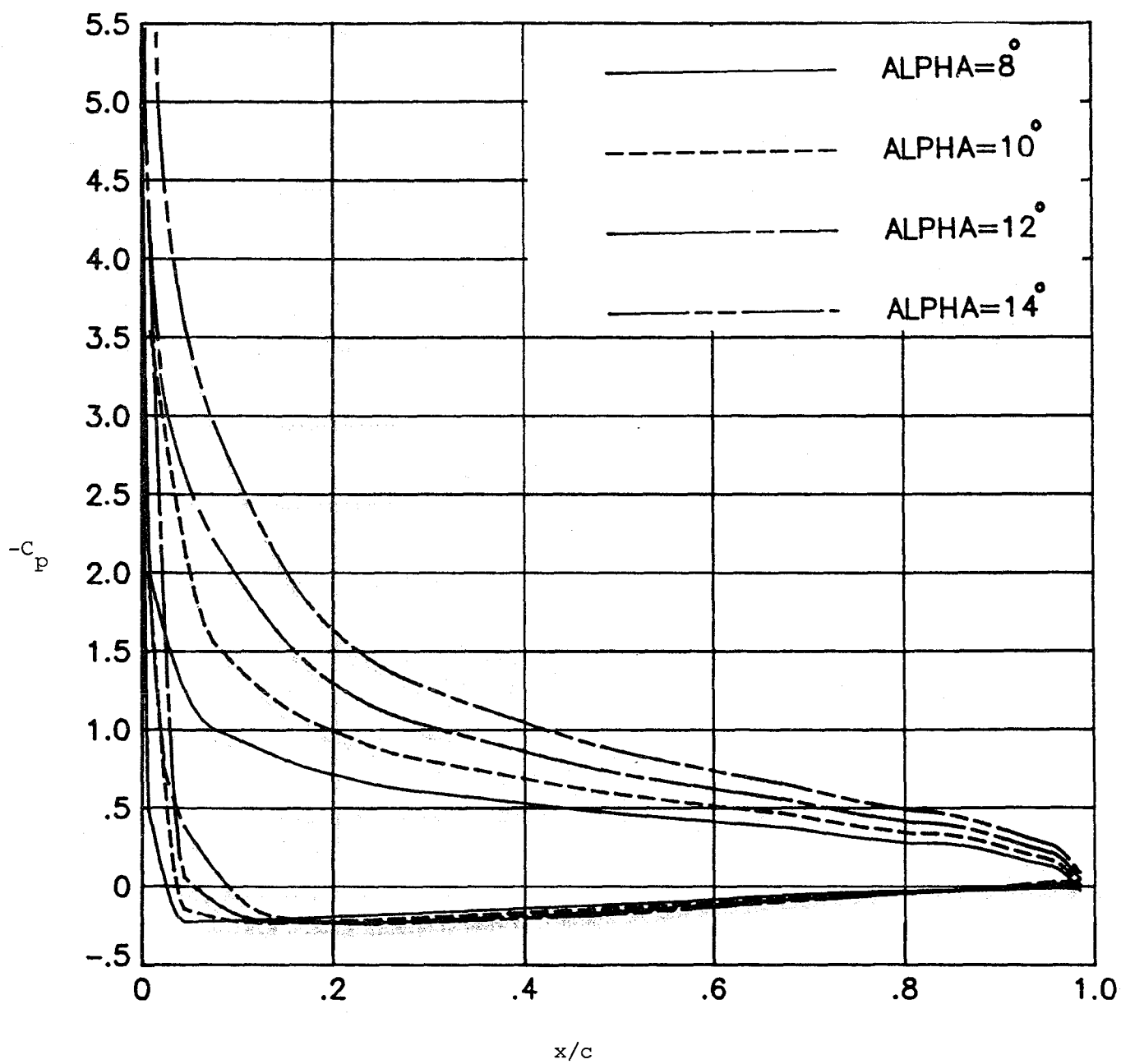
(e) $\eta = 0.911$

Fig. 13. Continued.
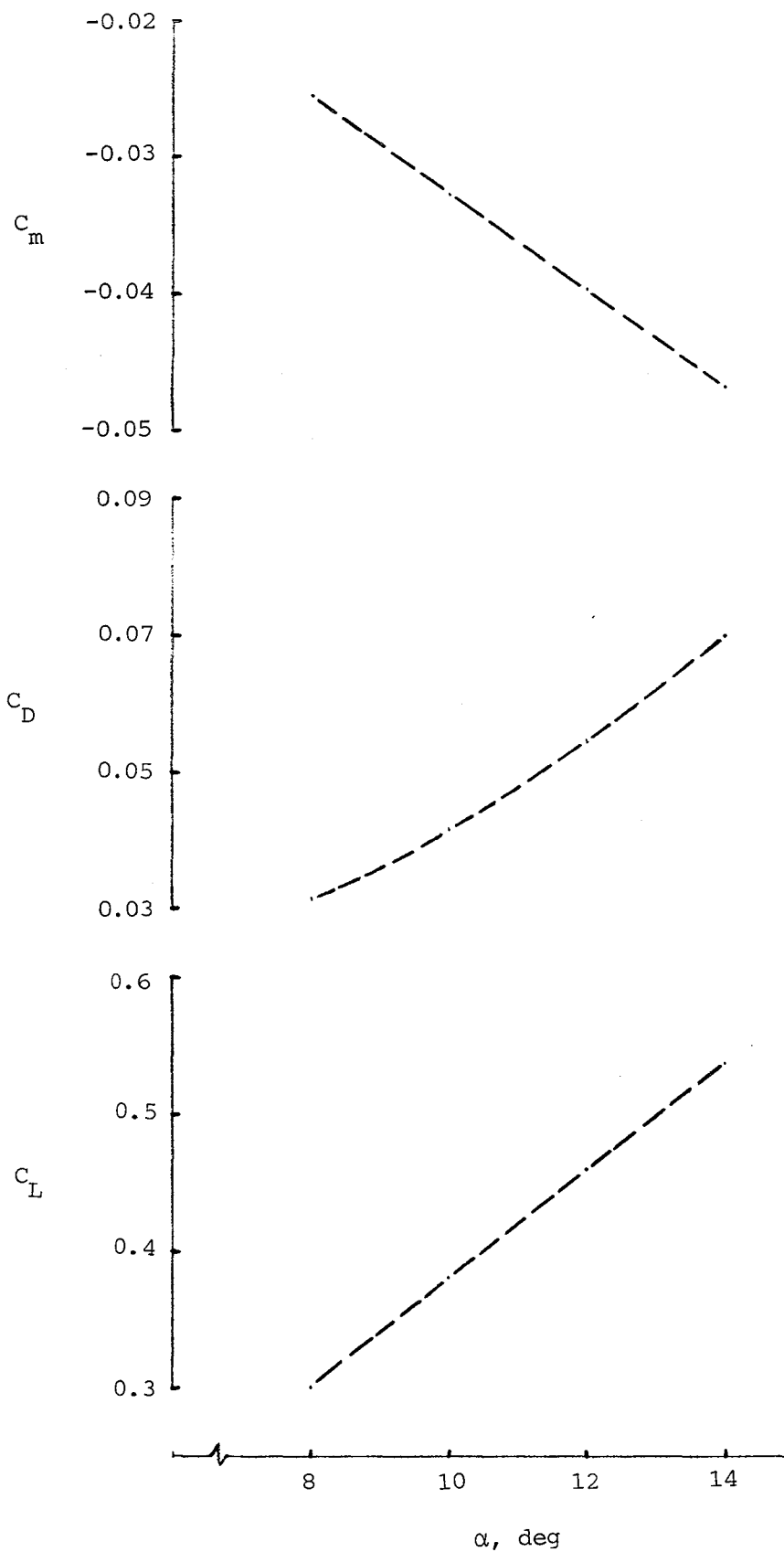
Fig. 14. Longitudinal aerodynamic characteristics for the basic
F-106B configuration; M_∞ = 0.08.

→ unit velocity vector

$\alpha = 8^\circ$

$\alpha = 14^\circ$
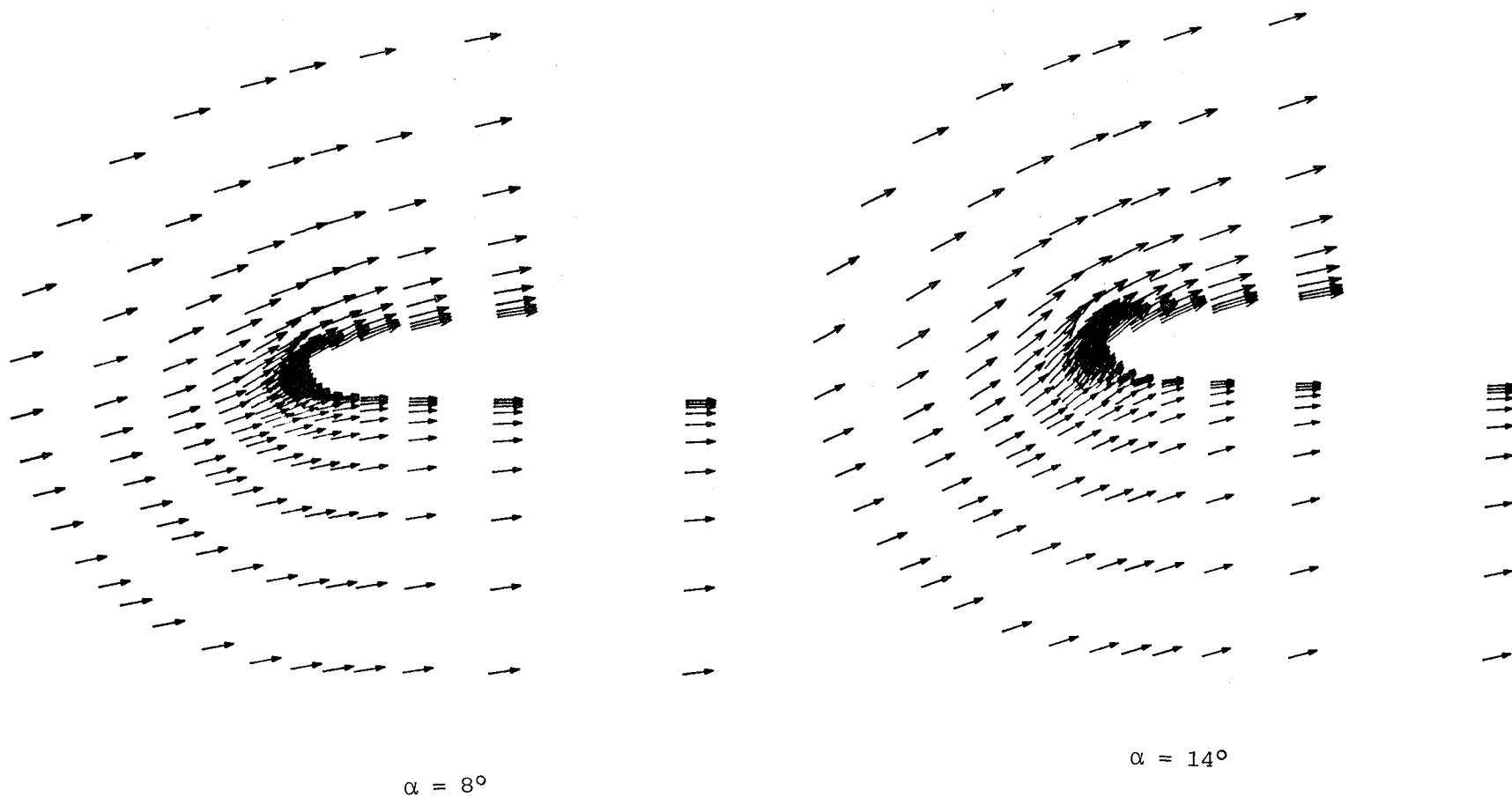
Fig. 15.   Wing leading-edge velocity field for the basic F-106B configuration
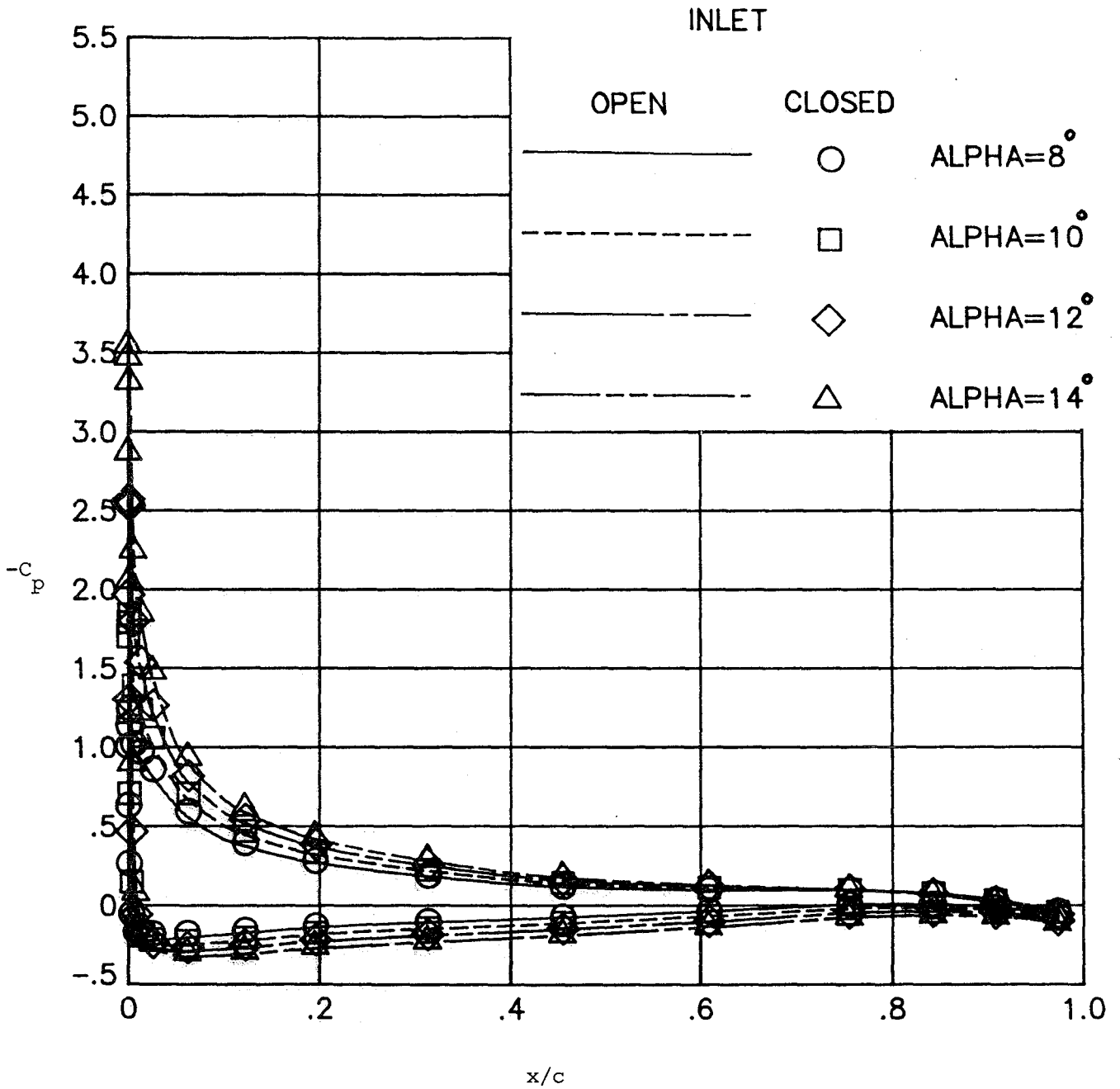at two angles of attack; $\eta = 0.24$, $M_\infty = 0.08$.

34
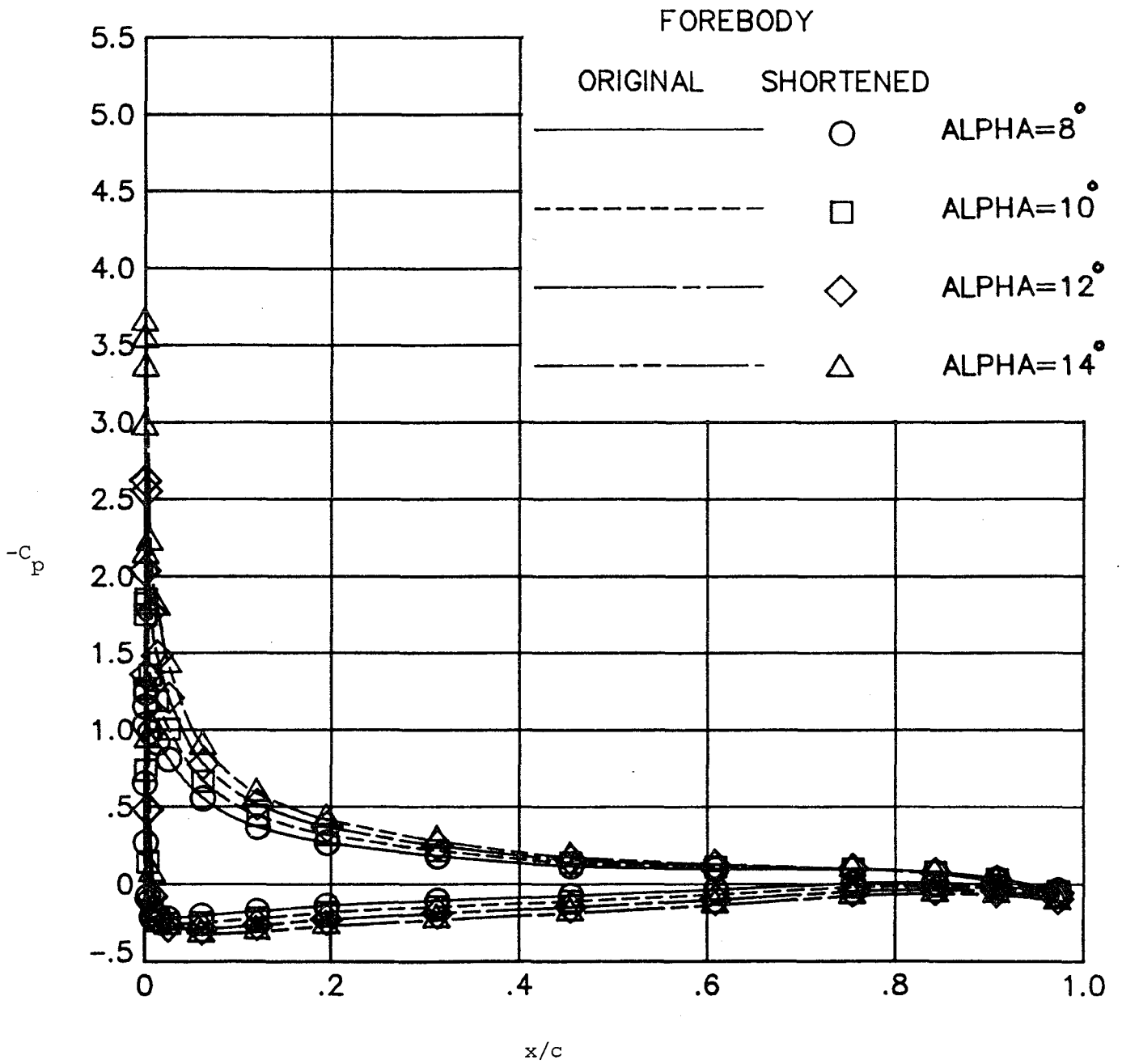
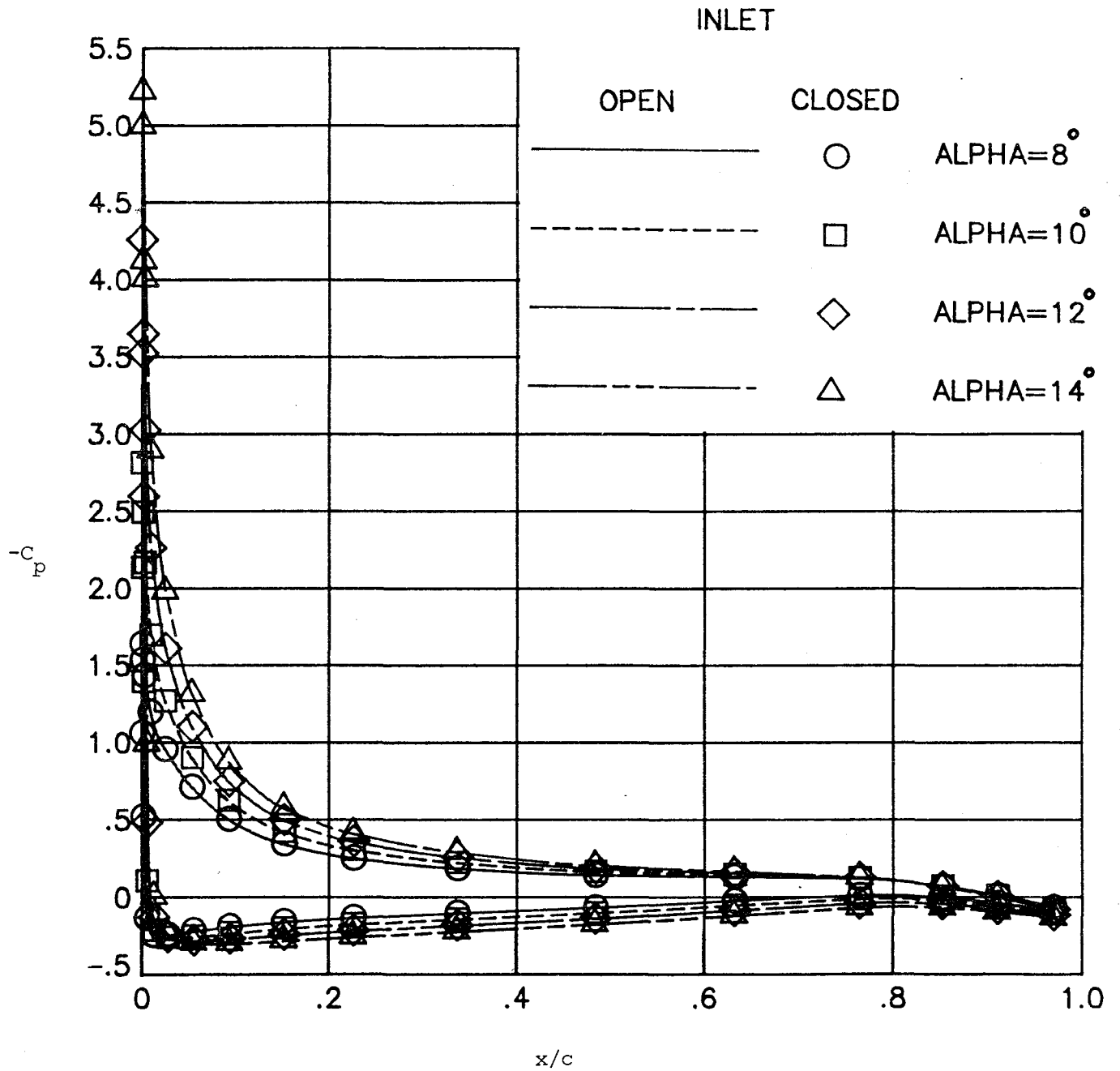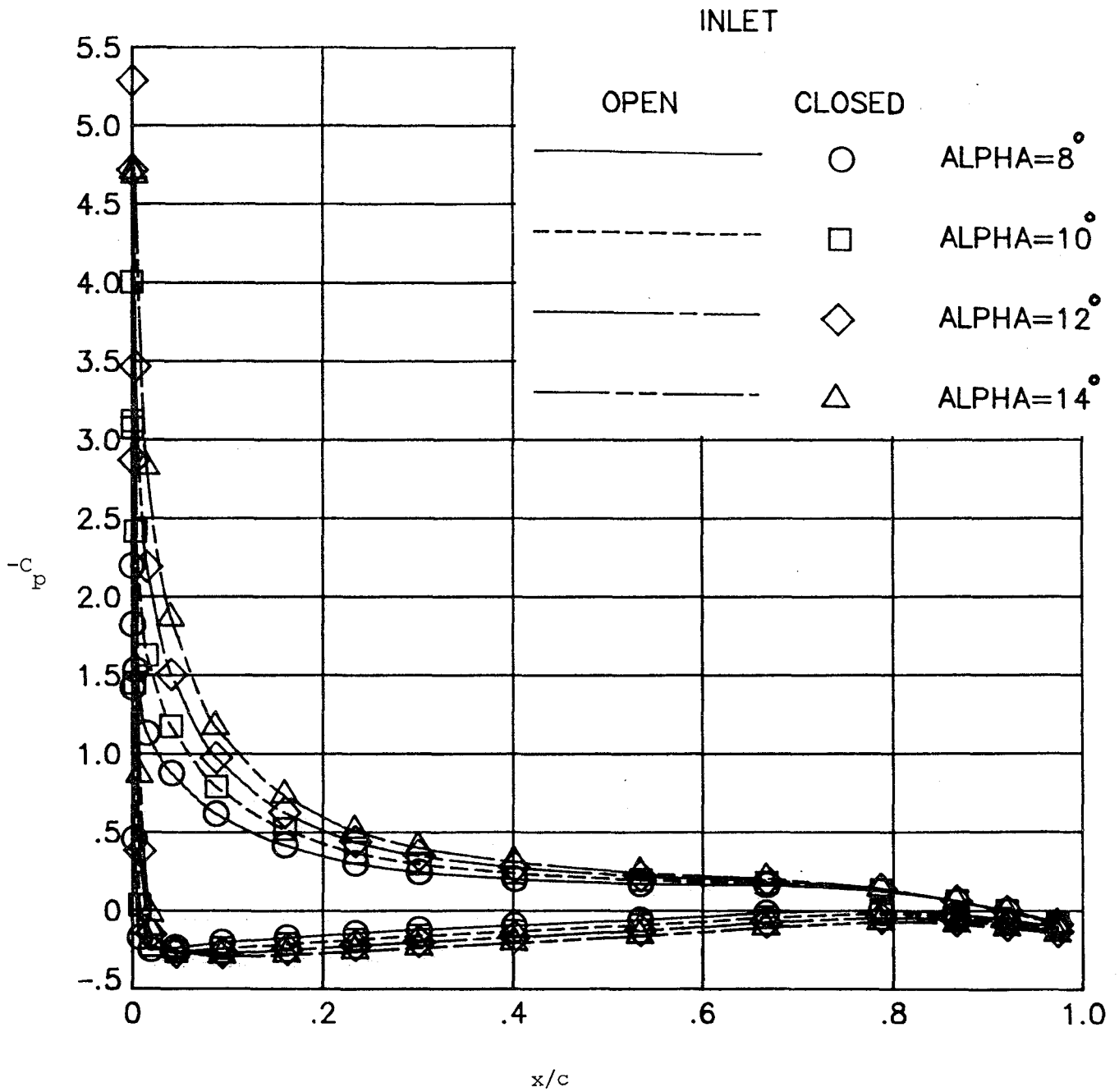(a) $\eta = 0.225$

Fig. 16.   Effect of forebody on the wing chordwise pressures at
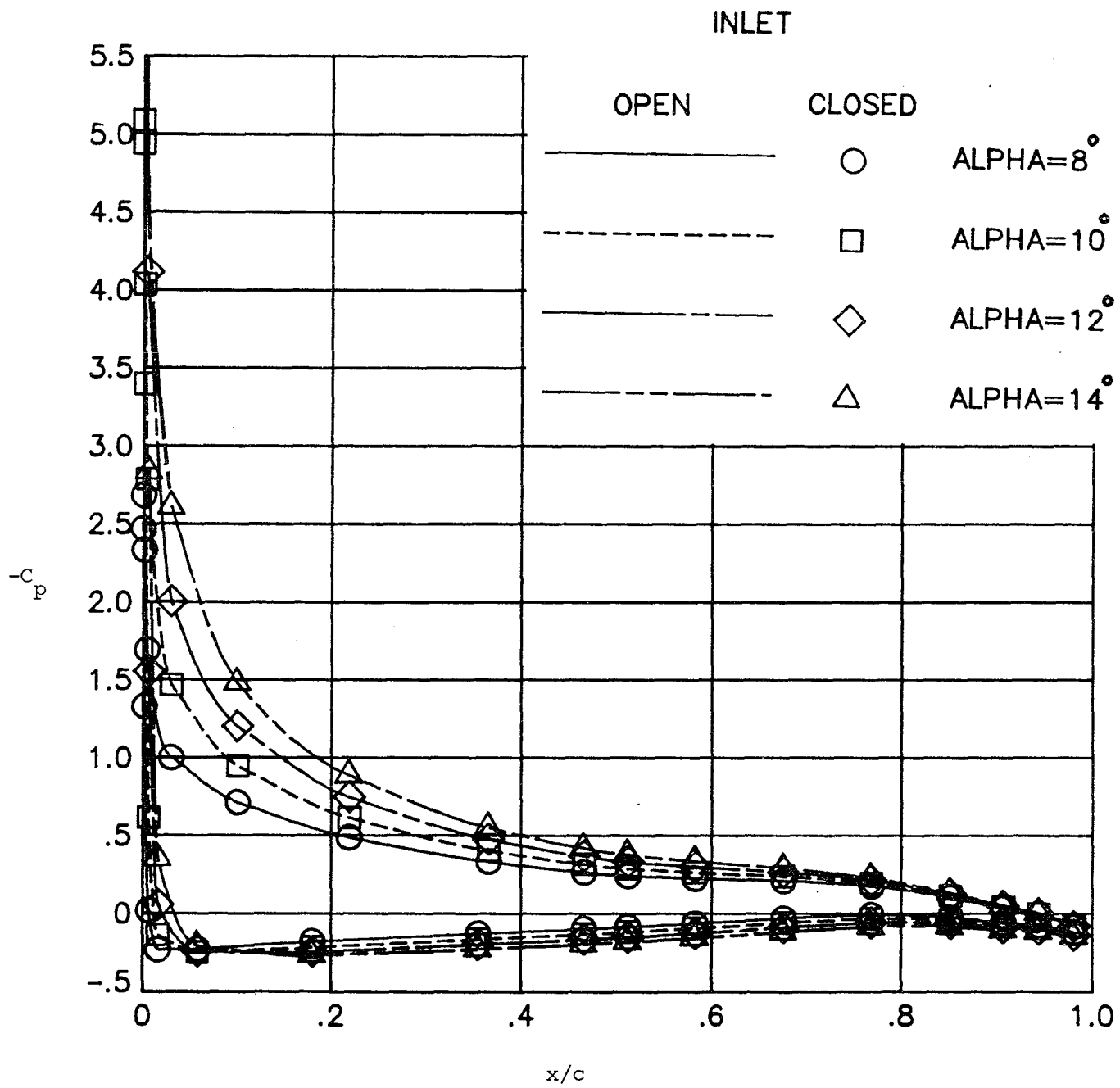   four angles of attack; $M_\infty = 0.08$.
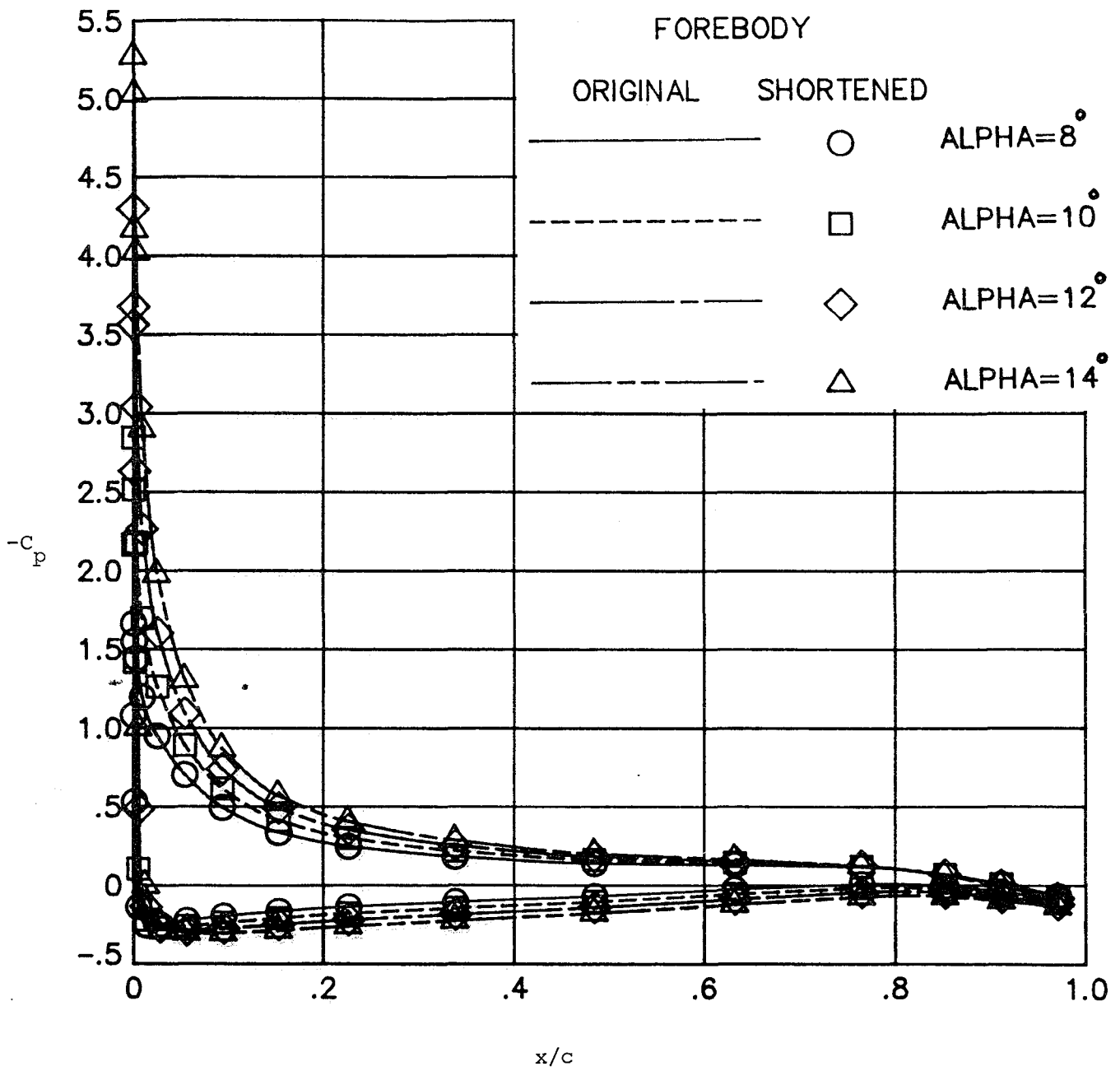
(b) η = 0.335
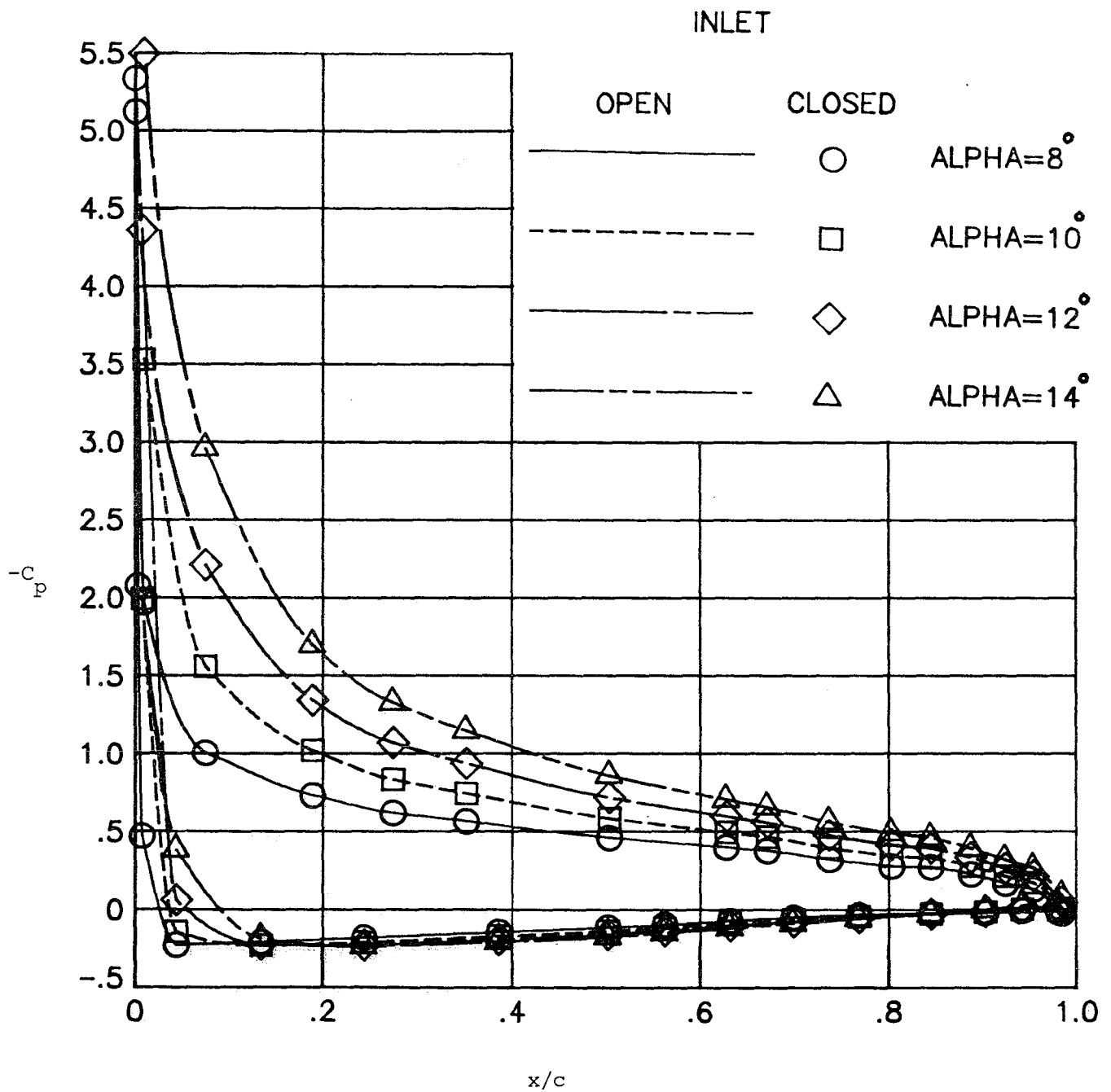
Fig. 16. Continued.
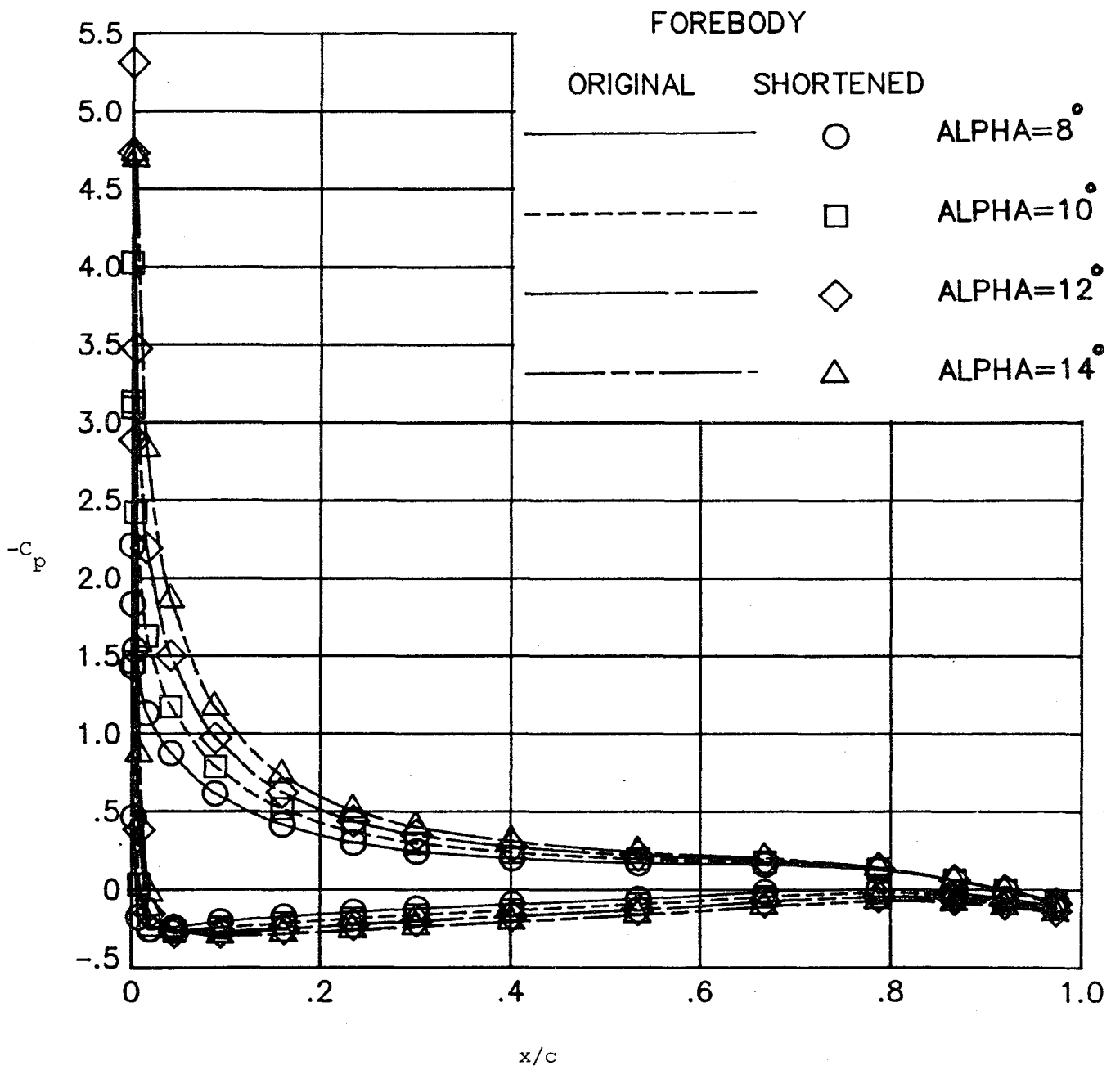
(c) $\eta = 0.469$

Fig. 16. Continued.
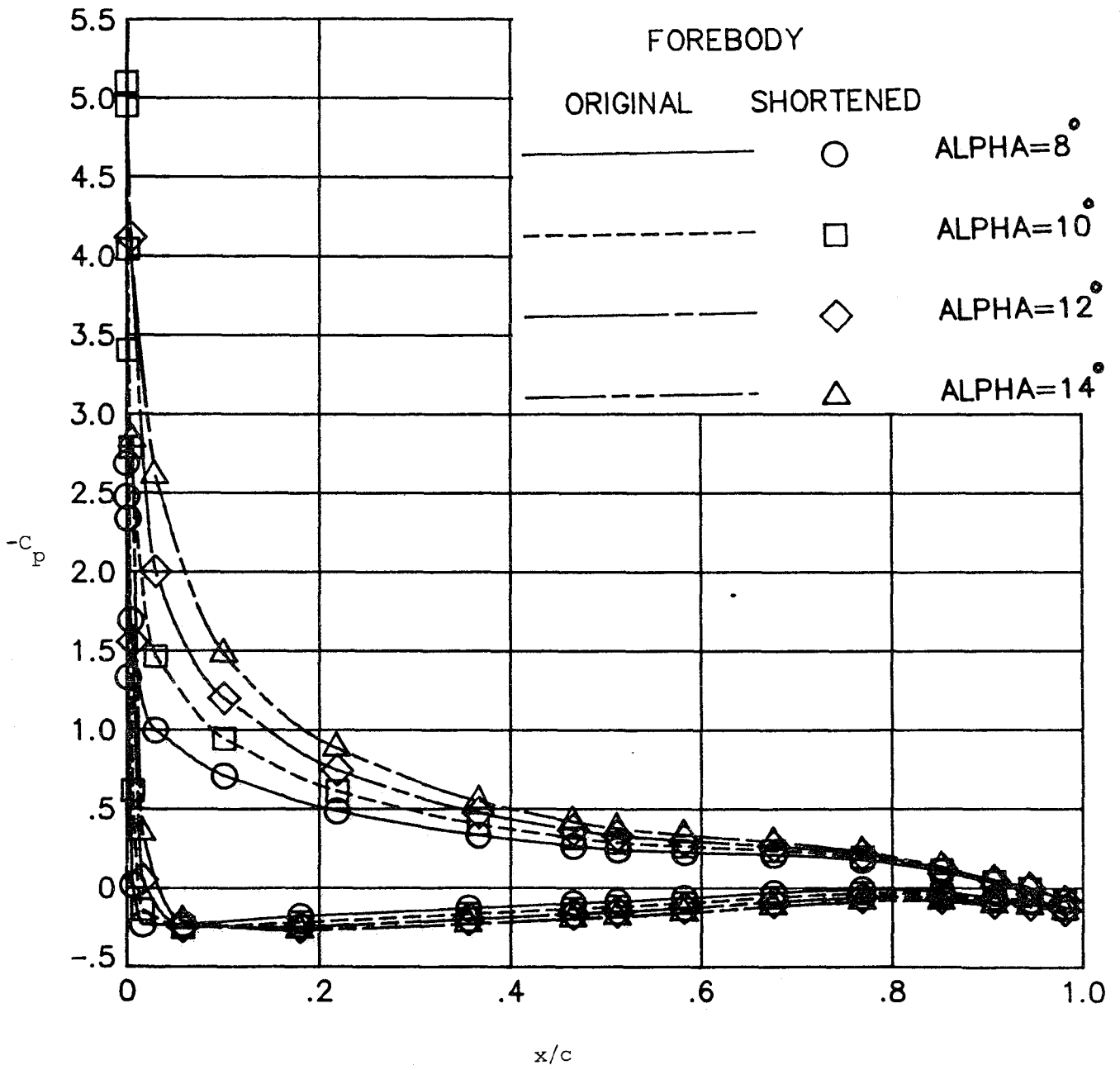
(d) $\eta = 0.666$

Fig. 16. Continued.
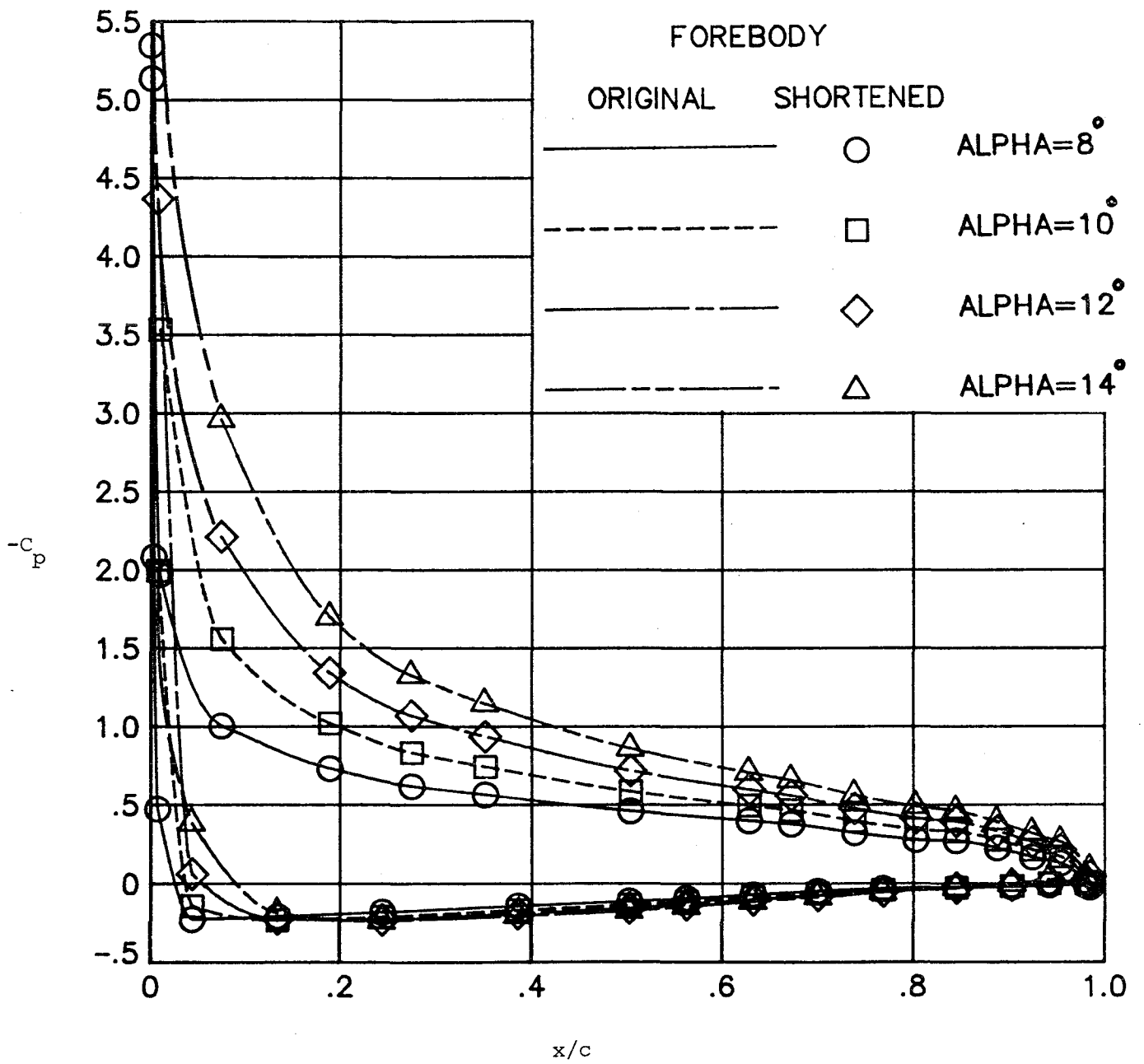
(e) $\eta = 0.911$

Fig. 16. Continued.
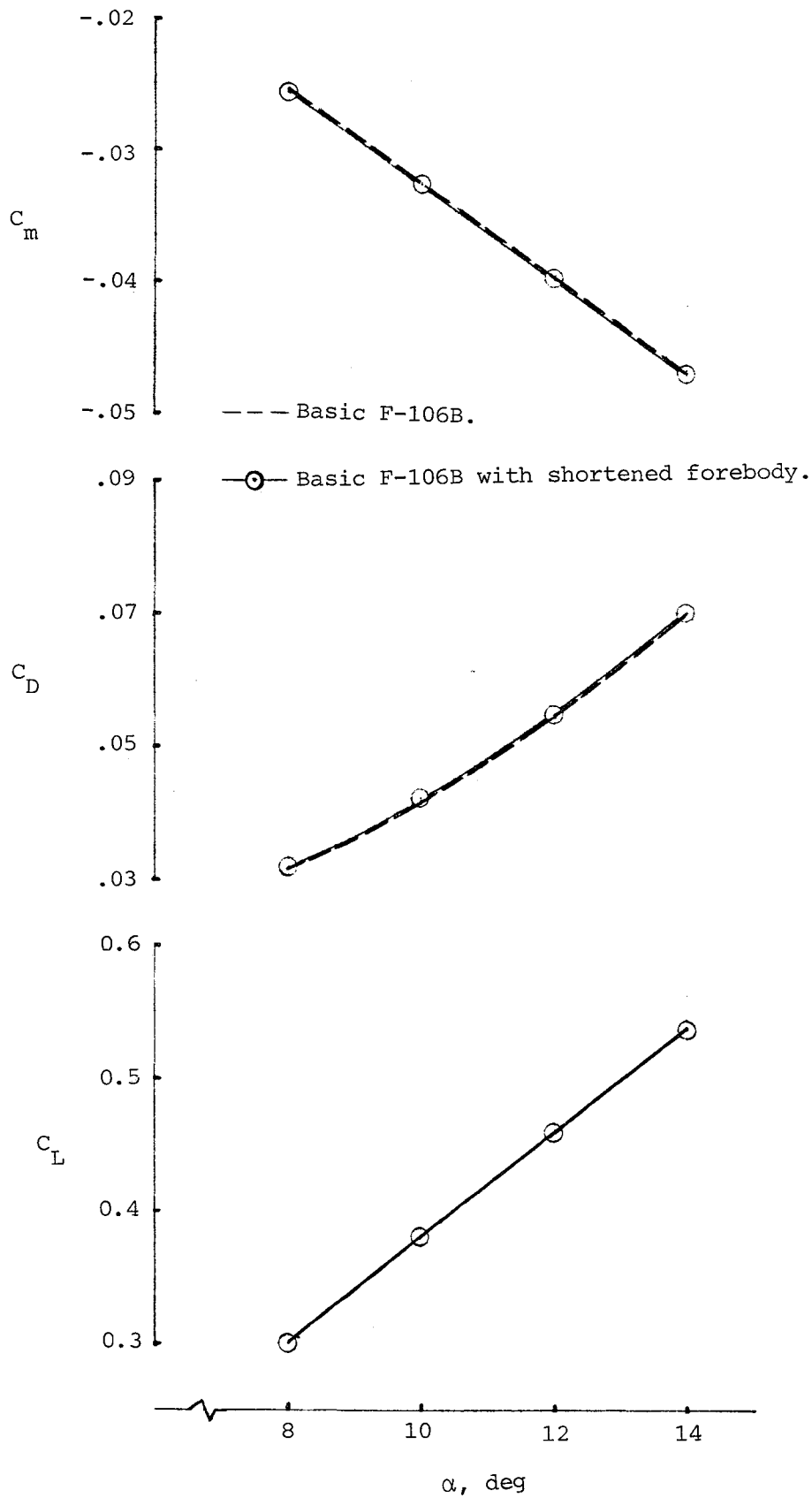
Fig. 17. Effect of forebody on longitudinal aerodynamic characteristics, $M_\infty = 0.08$.

Fig. 18. Wing leading-edge velocity field for the basic F-106B with shortened forebody at two angles of attack, $\eta = 0.24$, $M_\infty = 0.08$.

$\alpha = 14^o$

$\alpha = 8^o$

unit velocity vector

(a) η = 0.225
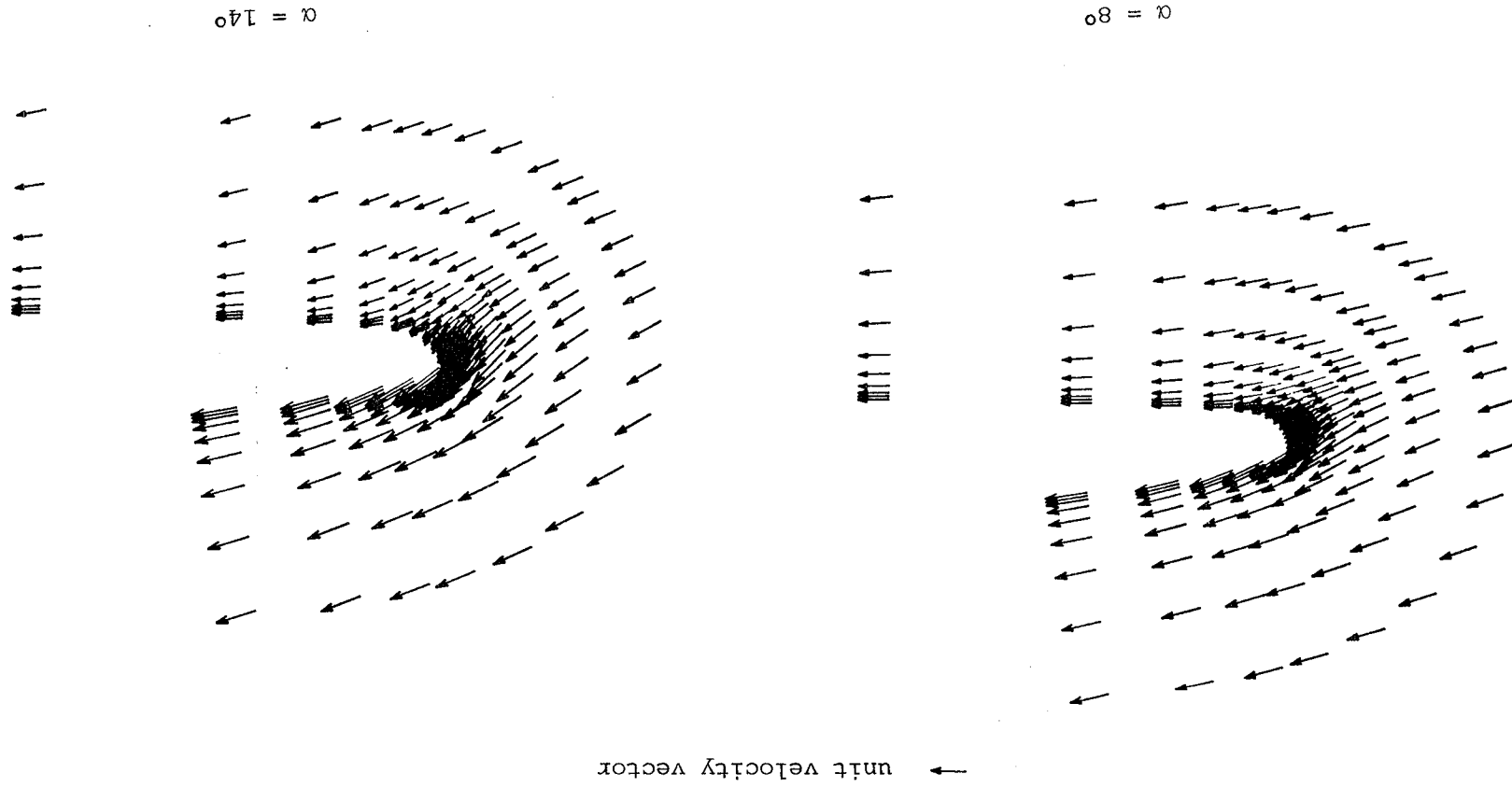
Fig. 19. Effect of inlet flow on the wing chordwise pressures at four angles of attack; M_∞ = 0.08.

(b) $\eta = 0.335$

Fig. 19. Continued.

43

(c) η = 0.469

Fig. 19. Continued.

44

INLET

OPEN   CLOSED

○ ALPHA=8°

□ ALPHA=10°

◇ ALPHA=12°

△ ALPHA=14°

(d) η = 0.666

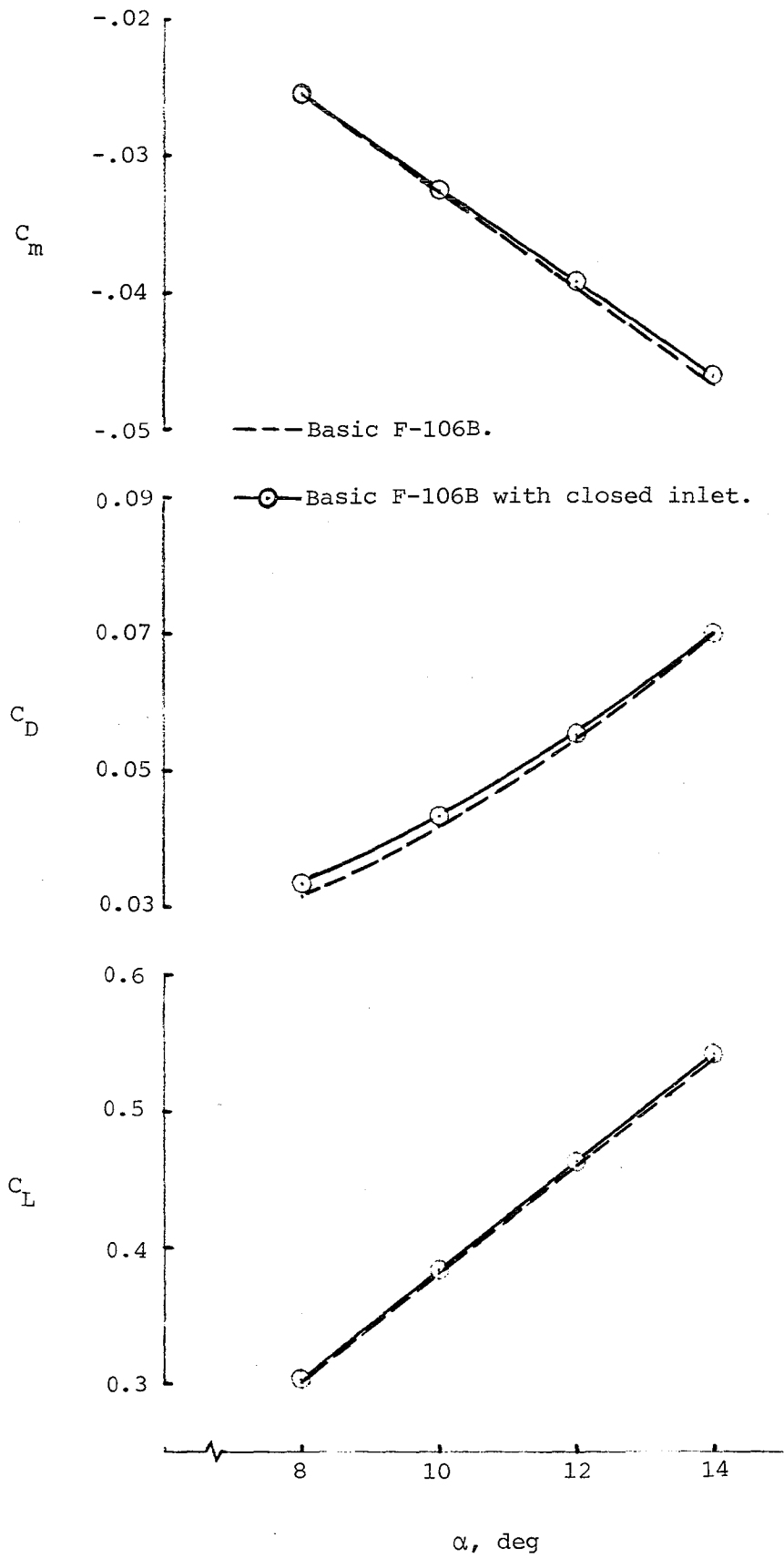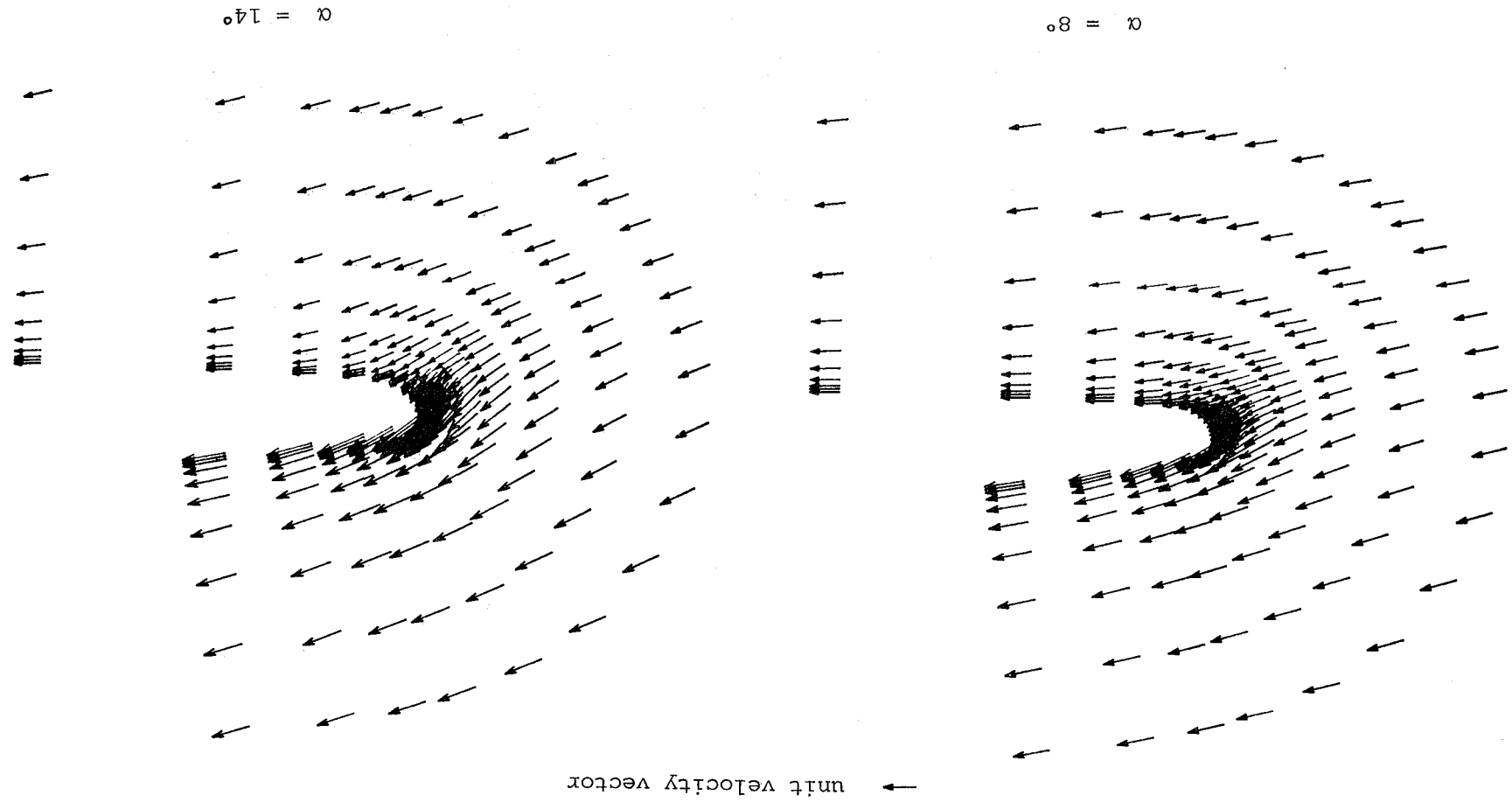Fig. 19. Continued.

45

(e) $\eta = 0.911$

Fig. 19. Continued.

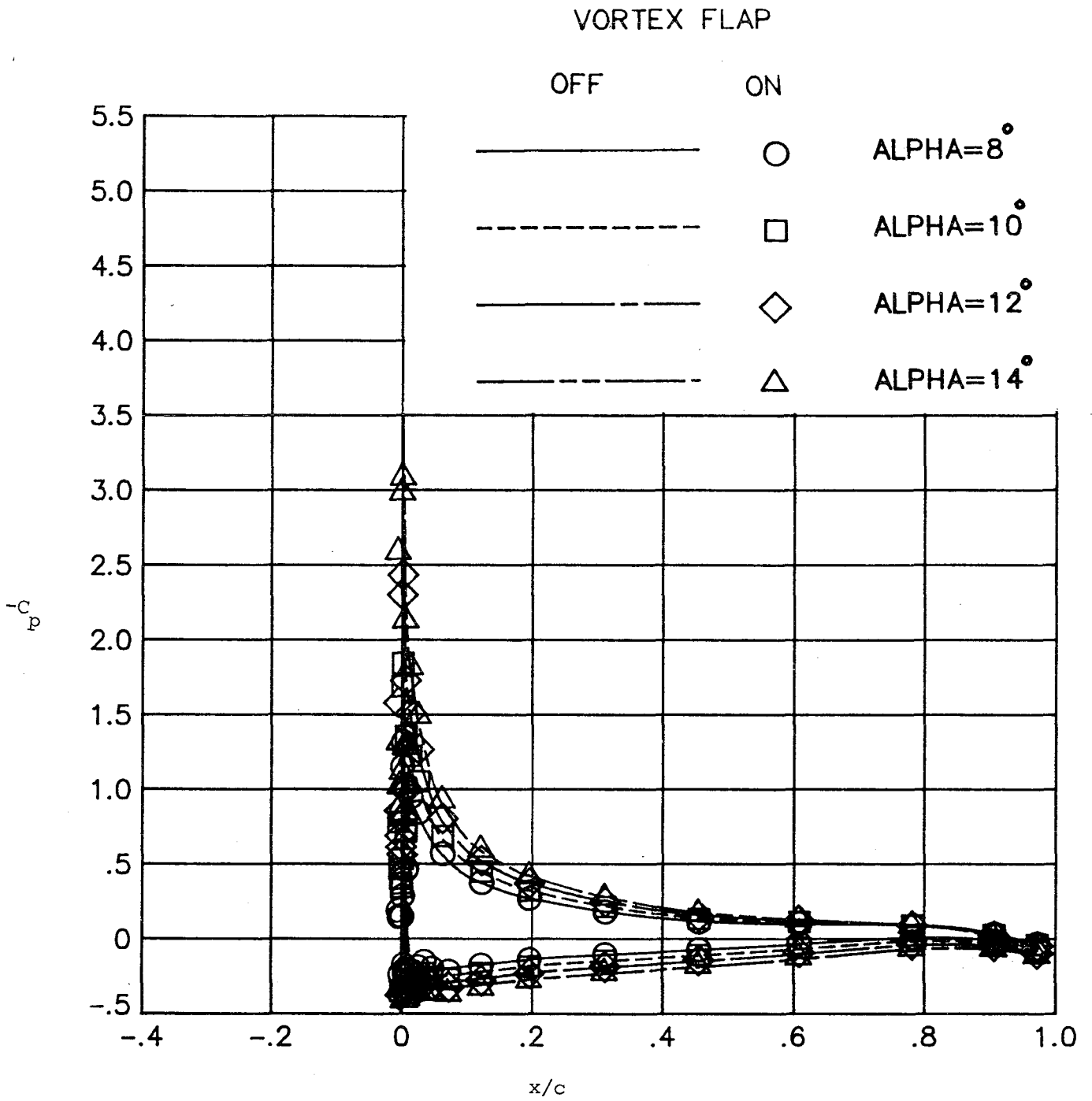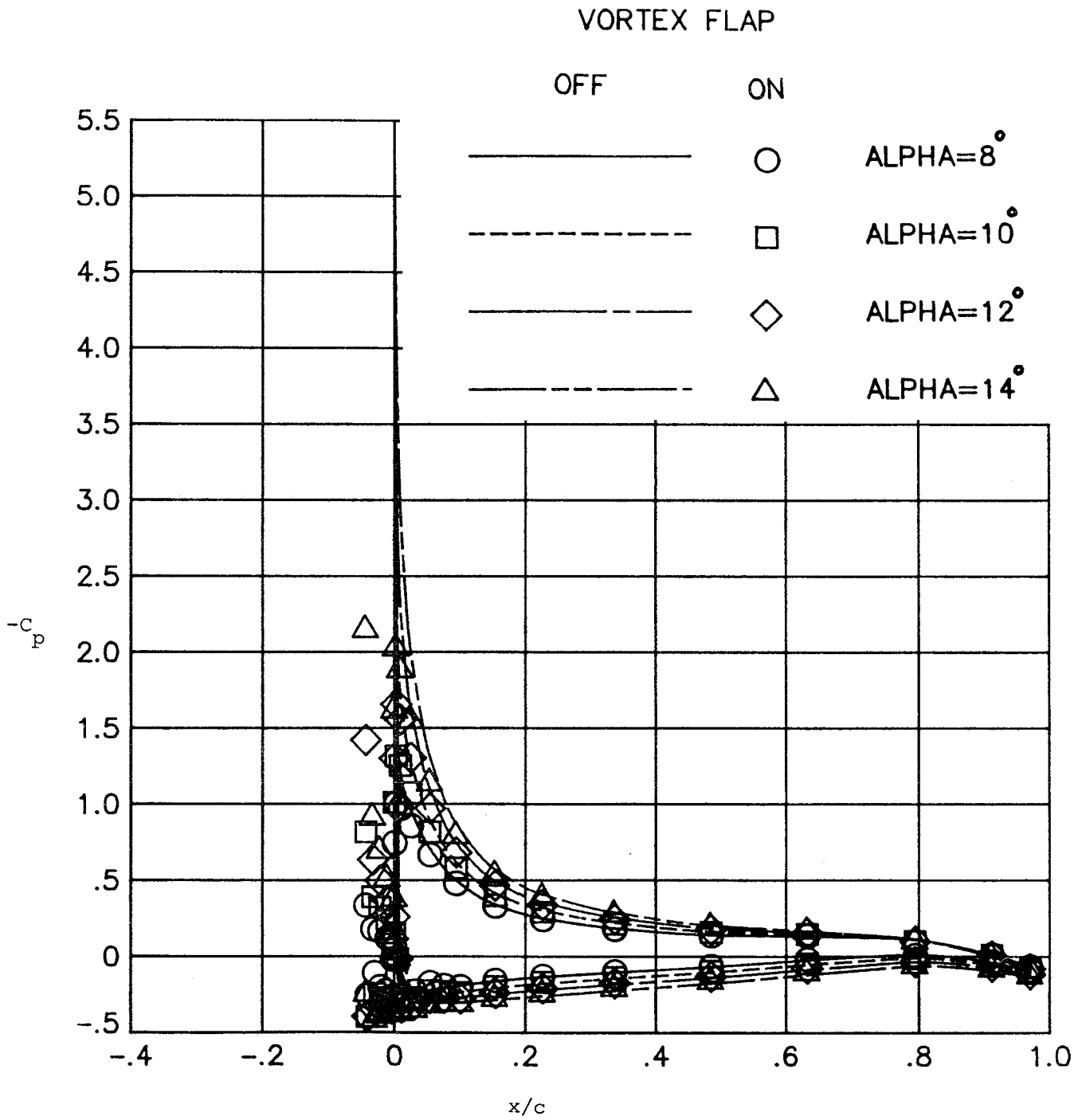Fig. 20. Effect of inlet flow on longitudinal aerodynamic
characteristics, $M_\infty = 0.08$.

Fig. 21. Wing leading-edge velocity field for the basic F-106B with closed inlet at two angles of attack, η = 0.24, $M_\infty = 0.08$.
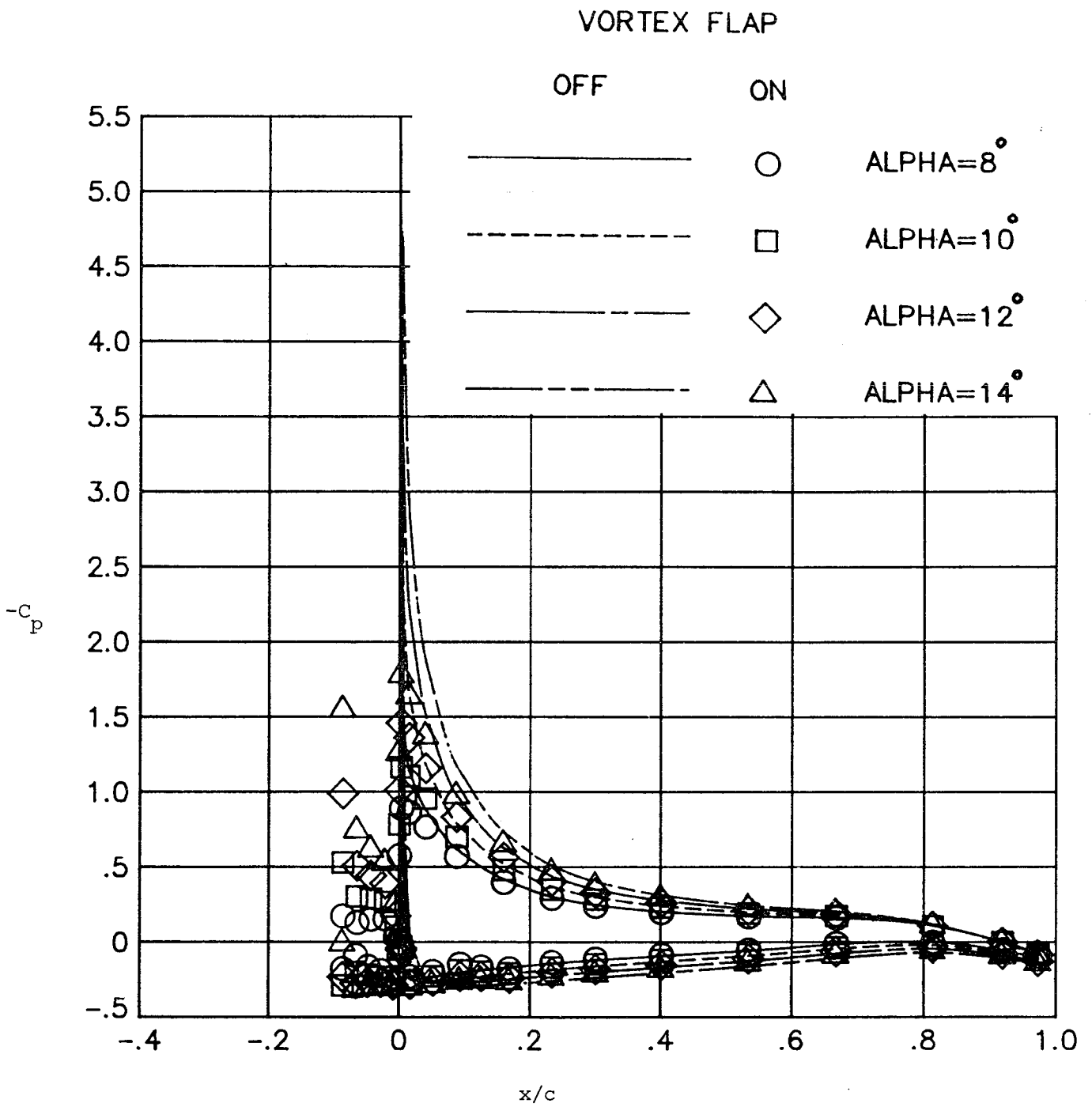
α = 14°

α = 8°

unit velocity vector ⟵

48

Fig. 22. Effect of vortex flap on the wing chordwise pressures at four angles of attack; M_∞ = 0.08.

(a) η = 0.225

VORTEX FLAP
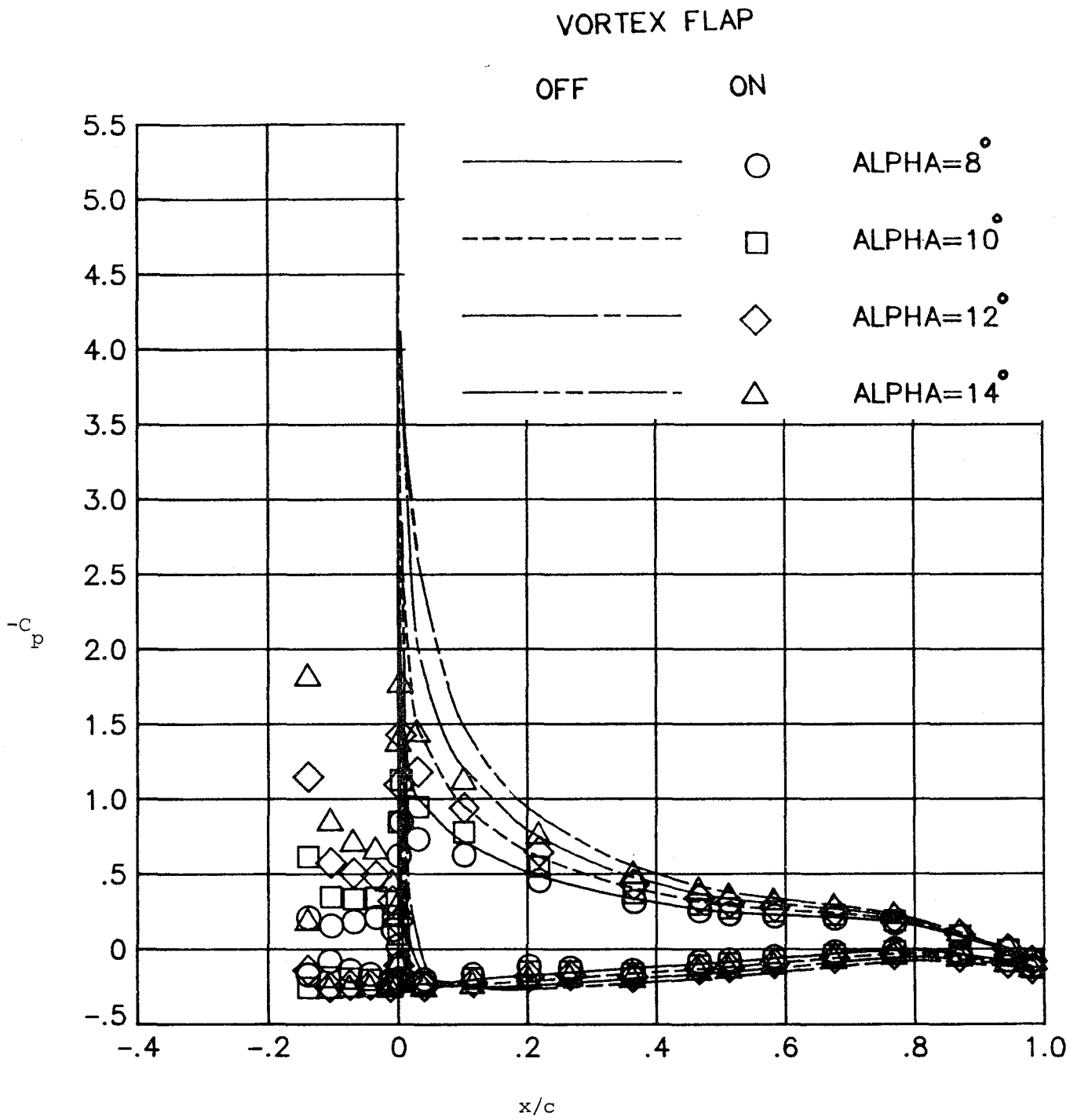
(b) η = 0.335

Fig. 22. Continued.

VORTEX FLAP

(c) η = 0.469

Fig. 22. Continued.

VORTEX FLAP

(d) η = 0.666

Fig. 22. Continued.
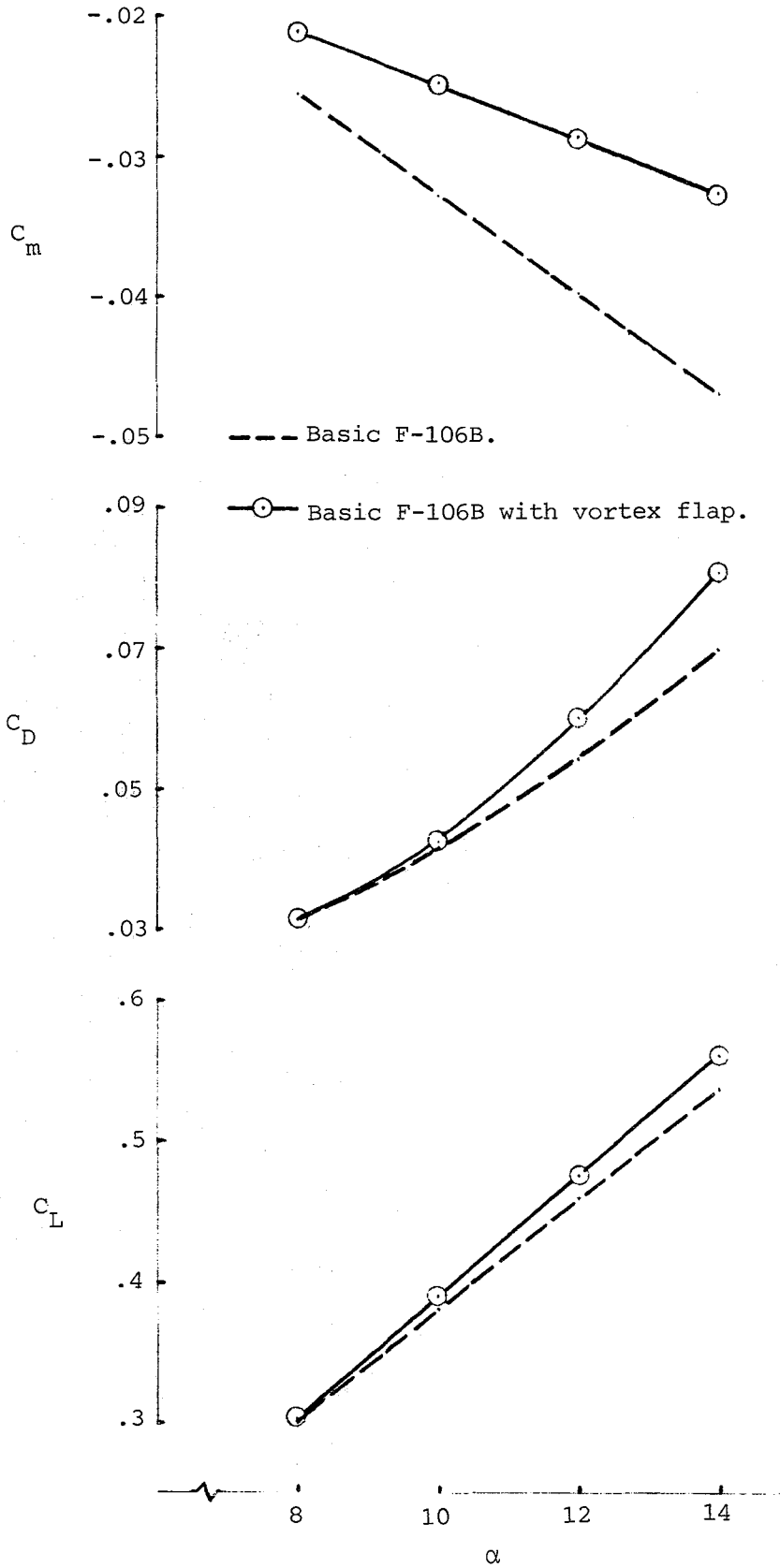
VORTEX FLAP

(e) η = 0.911

Fig. 22. Continued.

53

Fig. 23. Effect of vortex flap on longitudinal aerodynamic
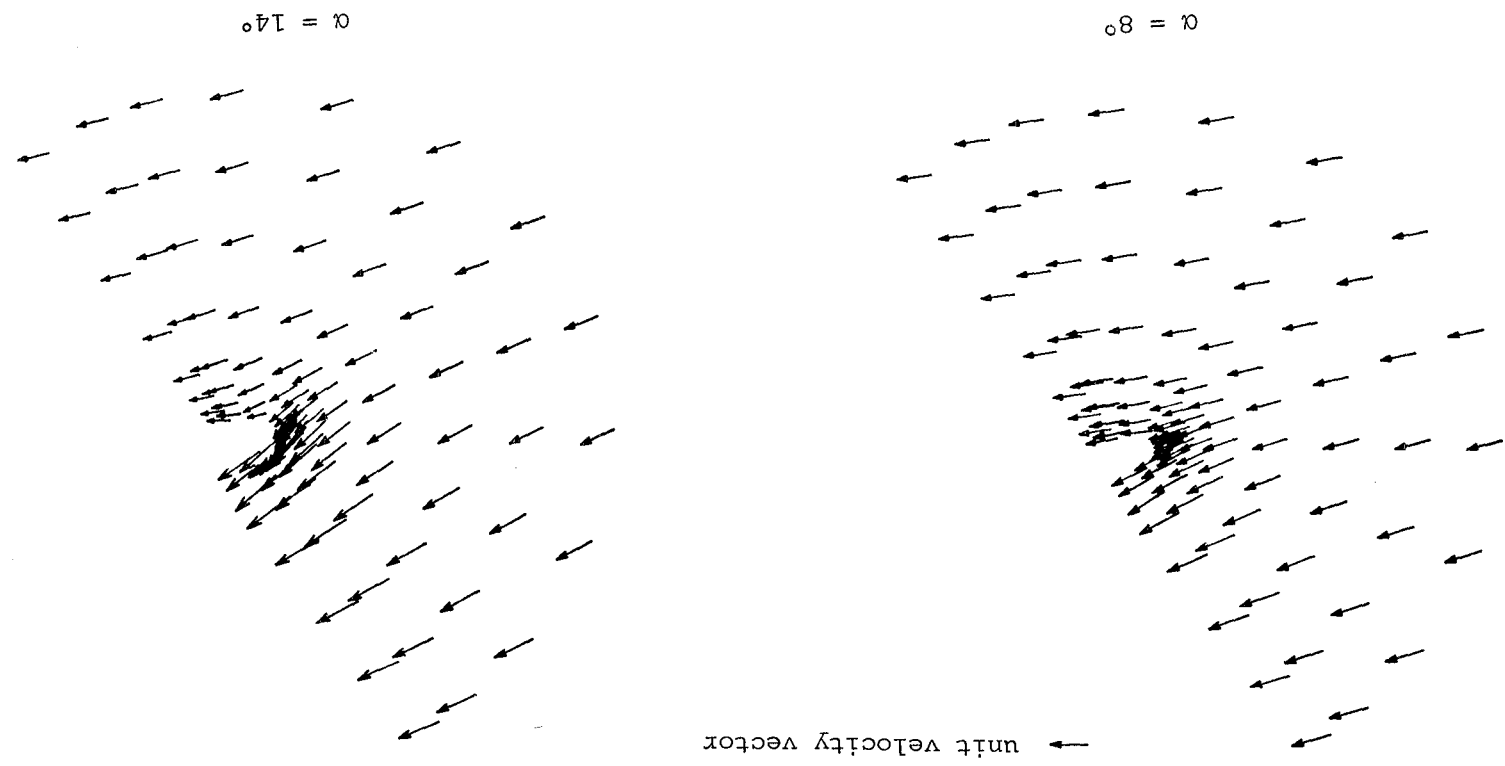characteristics; $M_\infty = 0.08$.

Fig. 24. Vortex flap leading-edge velocity field at two angles of attack, $\eta = 0.24$, $M_\infty = 0.08$.

$\alpha = 14°$

$\alpha = 8°$

← unit velocity vector

1. Report No. NASA CR-178165	2. Government Accession No.	3. Recipient's Catalog No.
4. Title and Subtitle PAN AIR APPLICATION TO THE F-106B		5. Report Date August 1986
		6. Performing Organization Code
7. Author(s) Farhad Ghaffari		8. Performing Organization Report No.
		10. Work Unit No.
9. Performing Organization Name and Address Vigyan Research Associates, Inc. 30 Research Drive Hampton, VA 23666-1325		11. Contract or Grant No. NAS1-17919
		13. Type of Report and Period Covered Contractor Report
12. Sponsoring Agency Name and Address National Aeronautics and Space Administration Washington, DC 20546		14. Sponsoring Agency Code 505-60-21-02

15. Supplementary Notes

Langley Technical Monitor: John E. Lamar

16. Abstract

The PAN AIR computer code was employed in the present study to investigate the aerodynamic effects of the various geometrical changes and flow conditions on a configuration similar to the F-106B half-airplane tested in the Langley 30×60-foot wind tunnel. The various geometries studied included two forebodies (original and shortened), two inlet flow conditions (open and closed) and two vortex flap situations (off and on). The attached flow theoretical solutions were obtained for Mach number of 0.08 and angles of attack of $8°$, $10°$, $12°$, and $14°$.

In general this investigation revealed that the shortening of the forebody or closing of the inlet produced only a small change in the overall aerodynamic coefficients of the basic F-106B configuration throughout the examined angles of attack. However, closing the inlet of the configuration resulted in a slightly higher drag level at low angles of attack. Furthermore, at and above $10°$ angle of attack, it was shown that the presence of the vortex flap causes an increase in the total lift and drag. Also, these theoretical results showed the expected reduction in longitudinal stability level with addition of the vortex flap to the basic F-106B configuration.

17. Key Words (Suggested by Author(s)) PAN AIR F-106B Inlet Flow Leading-Edge Vortex Flap	18. Distribution Statement Unclassified-Unlimited Subject Category 02		
19. Security Classif. (of this report) Unclassified	20. Security Classif. (of this page) Unclassified	21. No. of Pages 59	22. Price A04

End of Document